Journal
of
The Franklin Institute
Devoted to Science and the Mechanic Arts

Vol. 267 MARCH, 1959 No. 3

THE IONOSPHERIC FARADAY EFFECT AND ITS APPLICATIONS

BY

FRED B. DANIELS[1] AND SIEGFRIED J. BAUER[1]

ABSTRACT

An outline is given of the theory of the ionospheric Faraday effect (the rotation of the plane of polarization of radio waves by the ionosphere). Measurements of ionospheric characteristics by means of lunar radio reflections and radio transmissions from artificial satellites utilizing this effect are discussed. The rate of fading of satellite signals due to the Faraday effect is found to depend upon both the integrated electron density up to the height of the satellite and the local electron density at the satellite. Thus, a possibility exists of determining both quantities provided the satellite transmissions are received simultaneously by two or more stations. Expressions for the fading rate are derived and the effects of orbital parameters on the determination of ionospheric characteristics are discussed.

INTRODUCTION

Within the last few years radio reflections from the moon and, more recently, radio transmissions from artificial satellites have been used to measure ionospheric characteristics above the F-layer maximum, a region inaccessible to observation by vertical-incidence soundings. Since the Faraday effect (the rotation of the plane of polarization by the ionosphere) is usually made the basis of these measurements, this paper has been prepared for the purpose of analyzing this effect in detail.

THEORY

Magneto-Ionic Splitting

A linearly polarized radio wave traveling through the ionosphere is equivalent to two components (the ordinary and extraordinary waves), which, in the general case, are elliptically polarized with opposite senses

[1] U. S. Army Signal Research and Development Laboratory, Fort Monmouth, N. J.

(Note—The Franklin Institute is not responsible for the statements and opinions advanced by contributors in the JOURNAL.)

of rotation, and which travel with different velocities. In examining the behavior of the two components, it is useful to distinguish between two cases: the longitudinal case, where the direction of propagation is parallel to the Earth's magnetic field, and the transverse case, where the direction of propagation is perpendicular to the field.

In the longitudinal case, if the wave frequency is sufficiently greater than the collision frequency of the ionospheric electrons, the major axes of the two ellipses are mutually perpendicular. Also, if the wave frequency is much greater than the gyromagnetic and plasma frequencies, the ellipses become circles, and the resultant of the two circularly polarized waves is linearly polarized. However, because the two components have different phase velocities, the plane of polarization of the resultant gradually rotates as the wave progresses through the ionosphere. This phenomenon is known as the ionospheric Faraday effect.

In the transverse case the two elliptical components degenerate into linearly polarized waves, one component always remaining parallel to the magnetic field and the other one perpendicular thereto. However, because the components travel with different velocities, the resultant gradually changes along the path from a linearly polarized wave to an elliptically polarized one, and finally to one which is circularly polarized. Then the sequence is reversed and the wave changes back to a linearly polarized one. Now, however, the plane of polarization of the resultant is perpendicular to the original direction. Each time that the resultant passes through the cycle described, there is a 90°-rotation of the linearly polarized resultant.

For frequencies above 20 mc and values of less than 80° for the angle between the propagation direction and the magnetic field, the polarization is nearly circular, and the Faraday rotation may be computed as follows: If λ_o and λ_e are the wavelengths corresponding to the two phase velocities v_o and v_e, and dr is an element of path length, the rotations of the two components are given by

$$\phi_o = 2\pi \frac{dr}{\lambda_o} \quad \text{and} \quad \phi_e = 2\pi \frac{dr}{\lambda_e}.$$

Figure 1 shows the relation between ϕ_o, ϕ_e, and $d\phi$, the angle through

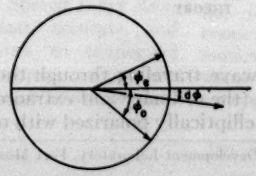

FIG. 1. Relation between phase vectors of magneto-ionic components.

which the plane of polarization rotates as the wave travels the distance dr. From this figure,

$$\phi_e + d\phi = \phi_o - d\phi$$

or

$$d\phi = \tfrac{1}{2}(\phi_o - \phi_e).$$

Substituting for ϕ_o and ϕ_e and expressing λ in terms of index of refraction n, angular frequency ω, and free space velocity c, and using the relations $\lambda = v/f$ and $n = c/v$, we have:

$$d\phi = \frac{\omega}{2c}(n_o - n_e)dr. \tag{1}$$

For frequencies sufficiently above the collision frequency and the plasma frequency $\left(\frac{\omega^2}{\omega_N^2} \gg 1\right)$ the Appleton-Hartree expression for the indices of refraction reduces to (1)[1]

$$n_{o,e}^2 = 1 - \frac{1}{\left(\frac{\omega}{\omega_N}\right)^2 - \frac{\omega_H^2}{2\omega_N^2}\sin^2\theta \pm \frac{\omega\omega_H}{\omega_N^2}\left[\left(\frac{\omega_H \sin^2\theta}{2\omega}\right)^2 + \cos^2\theta\right]^{1/2}}$$

where $\omega = 2\pi f$, the angular frequency of the transmitted wave, ω_N = angular plasma frequency, ω_H = angular gyromagnetic frequency and θ = angle between the direction of propagation and the Earth's magnetic field.

All practical cases can be treated by approximations of the Appleton-Hartree formula for the two limiting cases of longitudinal and transverse propagation (that is, $\theta = 0$ or $\theta = \pi/2$). The conditions under which quasi-longitudinal (QL) or quasi-transverse (QT) propagation prevails are given by:

$$\frac{\omega_H}{2}\sin\theta\tan\theta \ll \frac{\omega^2 - \omega_N^2}{\omega} \tag{QL}$$

and

$$\frac{\omega_H}{2}\sin\theta\tan\theta \gg \frac{\omega^2 - \omega_N^2}{\omega}. \tag{QT}$$

Faraday Effect for Quasi-Longitudinal Propagation

The approximation of the Appleton-Hartree formula that holds for the QL case is given by:

$$n_{o,e} = [1 - X/(1 \pm Y_L)]^{1/2} \simeq 1 - \frac{X}{2}(1 \mp Y_L) \tag{2}$$

[1] The boldface numbers in parentheses refer to the references appended to this paper.

where

$$X = \left(\frac{\omega_N}{\omega}\right)^2$$

$$Y_L = \frac{\omega_H}{\omega}\cos\theta$$

$$\omega_N^2 = \frac{4\pi e^2 N}{m}$$

$$\omega_H = \frac{e}{mc}B$$

N = electron density (cm^{-3})
e = electronic charge (esu)
m = electronic mass (gm), and
B = Earth's magnetic field (gauss).

Substituting in Eq. 2, we get:

$$n_o - n_e = \frac{\omega_N^2 \omega_H \cos\theta}{\omega^3}$$

and for Eq. 1:

$$d\phi_{QL} = \frac{e^3 BN\cos\theta}{2\pi m^2 c^2 f^2}\,dr. \tag{3}$$

Integration of Eq. 3 results in:

$$\phi_{QL} = \frac{e^3}{2\pi m^2 c^2 f^2}\int_0^R BN\cos\theta\, dr \tag{4}$$

where ϕ_{QL} is the total rotation along the propagation path from 0 to R.

The above expression gives the correct result for $d\phi$ only when the two components are circularly polarized. When θ is quite close to the limiting value that separates the QL and QT cases, the circles become ellipses, and when the eccentricity is large, $d\phi$ deviates from the value computed from Eq. 3. (In this case, $d\phi$ depends not only upon θ, but also upon the orientation of the plane of polarization of the incident wave relative to the plane containing the Earth's magnetic field and the direction of propagation.)

Faraday Effect for Quasi-Transverse Propagation

The approximation of the Appleton-Hartree formula that holds for the QT case is given by

$$n_{o,e} \simeq 1 - \frac{X}{2}\left(1 + \frac{Y_T^2}{2} \mp \frac{Y_T^2}{2}\right)$$

where

$$Y_T = \frac{\omega_H}{\omega} \sin \theta.$$

For this case, therefore,

$$n_o - n_e = \tfrac{1}{2} \cdot X Y_T^2$$

$$= \tfrac{1}{2} \cdot \frac{\omega_N^2 \omega_H^2}{\omega^4} \sin^2 \theta.$$

Substituting for ω_N and ω_H gives for Eq. 1

$$d\phi_{QT} = \frac{e^4 B^2 N}{8m^2 c^2 \pi^2 f^2} \sin^2 \theta dr \tag{5}$$

and integration of this expression results in

$$\phi_{QT} = \frac{e^4}{8m^2 c^2 \pi^2 f^2} \int_0^R B^2 N \sin^2 \theta dr \tag{6}$$

where ϕ_{QT} is the total rotation along the propagation path from 0 to R.

The above expression for the Faraday rotation is only formally true, since it assumes approximately circular polarization. The actual situation in the case of transverse propagation has been described above under the heading of "Magneto-Ionic Splitting," where it was pointed out that the polarization ellipses degenerate into lines, but the resultant gradually changes along the path from a line into a circle. This change occurs without any accompanying change in the orientation of the major axes of the ellipse. Therefore during this interval there is no directly observable change in the quantity ϕ. We may, however, interpret the transition from linear to circular polarization as being equivalent to a 45°-change in ϕ. This interpretation is reasonable because Eq. 5 gives $d\phi = \frac{\pi}{4}$ for a value of dr which can be shown to correspond to the change from a line to a circle. Furthermore, for a dr-value twice as great, the circle changes back to a line that is rotated 90° with respect to the original line.

The conditions under which the QL or QT approximations can be used have already been pointed out. It is also of interest to determine the relative magnitudes of the Faraday rotations for the two limiting cases: pure longitudinal and pure transverse propagation.

From Eqs. 3 and 5, setting $\theta = 0$ and $\theta = \pi/2$, respectively, the ratio of $d\phi_L$ to $d\phi_T$ becomes

$$\frac{d\phi_L}{d\phi_T} = \frac{4\pi mcf}{eB}.$$

For a frequency of 20 mc, the lowest frequency transmitted by the Russian satellites, this ratio is approximately equal to 30. The significance of this result is that as the satellite approaches the position for which the transverse case applies, the rate of fading will drop sharply. This drop can be seen in the fading curves of Australian satellite observations (2).

APPLICATIONS OF THE IONOSPHERIC FARADAY EFFECT

Moon Reflections

Murray and Hargreaves (3) first pointed out that the slow fading of lunar radio echoes is caused by the Faraday effect, and that the effect could be utilized to measure the integrated electron content in a vertical column of the ionosphere. Such measurements have been made by Brown *et al.* (4) and Evans (5) on two closely spaced frequencies. More recently the writers (6) determined the electron content from direct measurements of ϕ on a single frequency.

In moon-echo experiments, the frequencies used are usually considerably higher than the plasma frequency, the gyro frequency, and the collision frequency. The approximations made in deriving Eqs. 4 and 6 are therefore valid. Furthermore, at the locations where most of the experimental work has been done, the magnetic dip has a value such that the quasi-longitudinal expression for the Faraday rotation applies. Inasmuch as we are interested in determining the total electron content in a vertical column through the ionosphere, it is convenient to replace the path element dr by $dh \sec \delta$, where dh is a height element, and δ is the zenith angle of the propagation path within the ionosphere. If we make this substitution, put in the numerical values of the constants, and multiply by a factor of two to allow for the round-trip path, Eq. 4 becomes

$$\phi = 4.72 \times 10^4 \cdot f^{-2} \cdot \int_{h_1}^{h_2} NB \cos\theta \sec\delta dh \quad \text{(radians)}$$

where the limits of integration correspond to the region in which the ionization is large enough to make an appreciable contribution to the rotation. Since $B \cos\theta \sec\delta$ is essentially height-independent in the first 1000 km above the Earth's surface, this quantity can be taken out of the integral.[3] We can therefore write

$$\phi = 4.72 \times 10^4 \cdot f^{-2} B \cos\theta \sec\delta \int_{h_1}^{h_2} N dh$$

which is the equation that is customarily used in evaluating the results of lunar echo experiments (5, 6).

[3] Because of the substitution the expression for ϕ will be inaccurate close to the horizon.

Satellite Transmissions

For the one-way transmission from a satellite to the Earth, Eq. 4 becomes[4]

$$\phi = 2.36 \times 10^4 f^{-2} \cdot B \cos\theta \sec\delta \int_{h_1}^{h_s} N dh$$

where the upper limit of the integral (the height of the satellite) is now a function of time. To investigate the polarization fading that results when the signal is received with a linearly polarized antenna, we differentiate the above expression with respect to time. This results in

$$\frac{d\phi}{dt} = 2.36 \times 10^4 \cdot f^{-2} \cdot B \left\{ \frac{\partial}{\partial t} (\cos\theta \sec\delta) \int_{h_1}^{h_s} N dh + (\cos\theta \sec\delta) N_s \frac{dh_s}{dt} \right\} \quad \text{(radians/sec)} \quad (7)$$

where N_s is the electron density at the satellite. (In evaluating the derivative, the assumption is made that N is a function of h, but not of t.) In this expression, the effects of horizontal and vertical motion are separated, and the contributions of each of these components of motion may be estimated if information is known regarding the orbit.

The value of dh_s/dt can be obtained from the expression for the radius vector of an elliptical orbit:

$$r_s = \frac{a(1 - \epsilon^2)}{1 + \epsilon \cos\Psi}$$

where a is the semi-major axis of the orbit, r_s is the radius vector, ϵ is the eccentricity of the orbit, and Ψ the angular variable. For dh_s/dt we therefore have

$$\frac{dh_s}{dt} = \frac{dr_s}{dt} = \frac{\epsilon a(1 - \epsilon^2) \sin\Psi}{(1 + \epsilon \cos\Psi)^2} \frac{d\Psi}{dt} \simeq \frac{2\pi\epsilon a}{T} \sin\Psi$$

where T is the period of revolution.

This result shows that dh_s/dt varies sinusoidally from a value of zero at perigee and apogee to a maximum value of $2\pi\epsilon a/T$ when $\Psi = 90°$ and 270°, that is, at a height $h = a(1 - \epsilon^2) - r_e$, where r_e is the Earth's radius. (It should be noted that dh_s/dt changes sign in passing through

[4] Because of the approximations made in deriving Eq. 4, ϕ will be in error by about 20 per cent at 20 Mc (the lowest Russian satellite frequency); for higher frequencies this error will become progressively smaller.

perigee and apogee.) One practical conclusion that can be drawn from these considerations is that the second term in Eq. 7 approaches zero for an observer located near perigee or apogee. (It will also approach zero as the satellite moves outside of the ionosphere, or if the orbit is circular.) In the general case, however, the separation of the two terms in Eq. 7 may be difficult. This problem will be discussed in more detail below.

Since the radial velocity component u of the satellite with respect to the observer introduces a Doppler frequency shift which differs for the two magneto-ionic components, we should investigate the contribution of the Doppler effect to the Faraday rotation. Because of the Doppler shift the two components have the frequencies

$$f_o = f\left(1 + \frac{u}{c} n_o'\right)$$

and

$$f_e = f\left(1 + \frac{u}{c} n_e'\right)$$

where the primed indices of refraction refer to values at the satellite's location. Using these frequency values in the expression for the Faraday effect, we obtain

$$\begin{aligned} d\phi &= \tfrac{1}{2}(\phi_o - \phi_e) \\ &= \frac{\omega}{2c} dr \left[(n_o - n_e) + \frac{u}{c} (n_o n_o' - n_e n_e') \right] \end{aligned}$$

or

$$\simeq \frac{\omega}{2c} dr \left\{ (n_o - n_e) \left(1 + \frac{2u}{c}\right) \right\}$$

which shows that the error due to the Doppler effect is negligible, since $\frac{2u}{c}$ is small compared to unity.

In order to evaluate accurately the Faraday rotation we must eliminate the contribution of satellite spin to the observed fading. This is easily done if measurements are made on two transmitted frequencies which are sufficiently separated, because the Faraday rotation is inversely proportional to frequency, while the contribution of the spin is usually the same on both frequencies (depending upon the antenna configuration). (This discussion assumes that the propagation path is essentially the same at both frequencies.)

In considering the application of the Faraday effect to the determination of ionospheric parameters, we must examine the relative im-

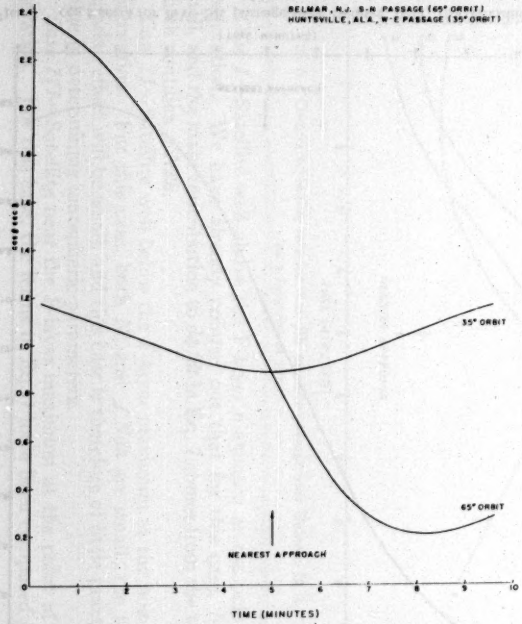

FIG. 2. $\cos\theta \sec\delta$ as a function of time for circular satellite orbits.

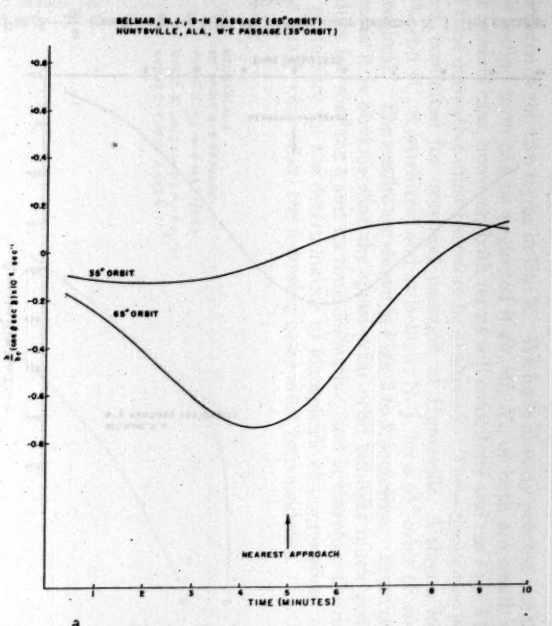

FIG. 3. $\frac{\partial}{\partial t}(\cos\theta \sec\delta)$ as a function of time for circular satellite orbits.

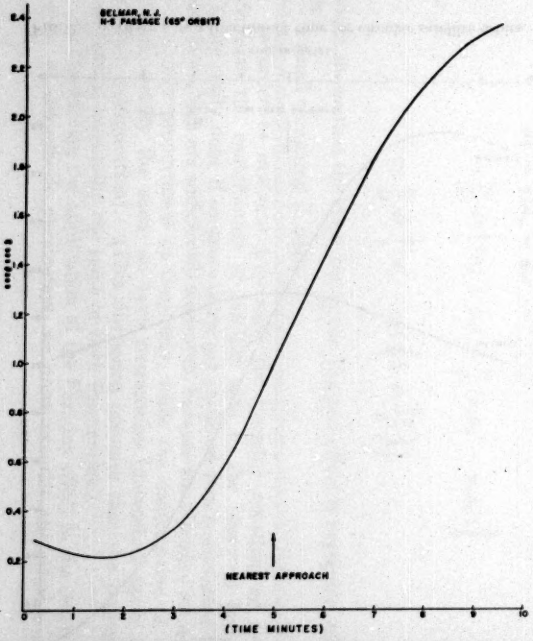

FIG. 4. $\cos\theta \sec\delta$ for NW–SE passage over Belmar, N. J. (for circular orbit).

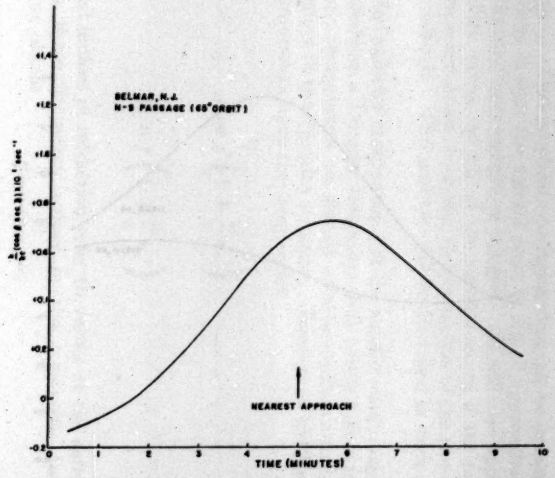

FIG. 5. $\frac{\partial}{\partial t}(\cos\theta \sec\delta)$ for NW–SE passage over Belmar, N. J. (for circular orbit).

V.26
1959

portance of the two terms in Eq. 7. We have already pointed out that the second term can be neglected if dh_s/dt, N_s, or both are small. In the general case, however, both terms will contribute and cos θ sec δ and its time derivative must therefore be evaluated. These quantities have been computed for overhead passages at Huntsville, Alabama for a 35°-orbit (U. S. satellites) and at Belmar, N. J. for a 65°-orbit (Russian satellites). The results are shown in Figs. 2 to 5, inclusive. From these figures it is obvious that the quasi-polar orbit exhibits much greater values for cos θ sec δ and its time derivative, and is therefore the orbit of preference for the determination of ionospheric characteristics. For the quasi-polar orbit, the following cases must be considered.

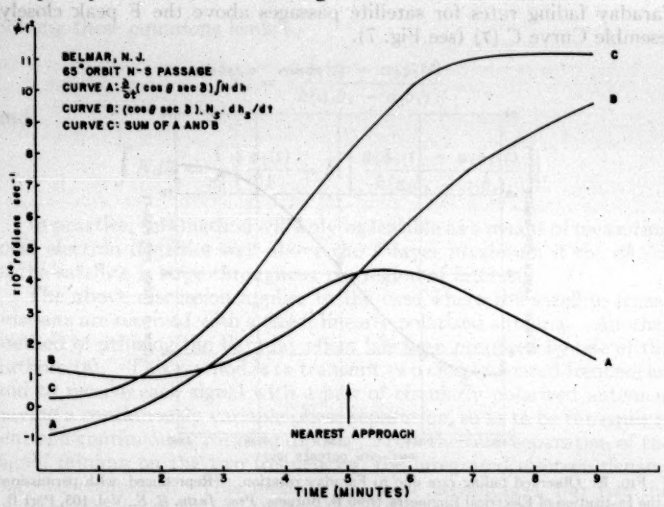

FIG. 6. Computed fading rate for NW–SE satellite passage over Belmar, N. J. as a function of time.

Case I—Satellite well above the F-layer maximum at the point of observation. We have already pointed out that for this case, N_s is small, and the main contribution to $d\phi/dt$ in Eq. 7 comes from the term which contains $\int N dh$.

Case II—Satellite well below the F-layer maximum at the point of observation. For this case, both N_s and $\int N dh$ are small; the total Faraday effect will be small, and this case is therefore of little practical value in determining ionospheric parameters.

Case III—Satellite near the F-layer maximum at the point of observation. For this case, the terms in Eq. 7 have been computed as a

function of time for an overhead passage at Belmar, N. J. The following conditions have been assumed: North to South passage, $h_s = 350$ km, $dh_s/dt = 5 \times 10^4$ cm/sec (a representative value for the orbit of Sputnik II), $N_s = 7 \times 10^5$ electrons cm^{-3}, and $\int Ndh = 5 \times 10^{12}$ electrons cm^{-2}. The results of this computation are shown in Fig. 6 in which the fading rate ϕ has been normalized with respect to frequency. Curve A shows the contribution of the term containing $\int Ndh$, and Curve B the contribution of the term containing N_s. It is obvious that the two terms, for the case assumed, are of approximately equal magnitude, and that the computed Faraday fading (Curve C) is the combined effect of these terms. It should be noted that observed Faraday fading rates for satellite passages above the F peak closely resemble Curve C (7) (see Fig. 7).

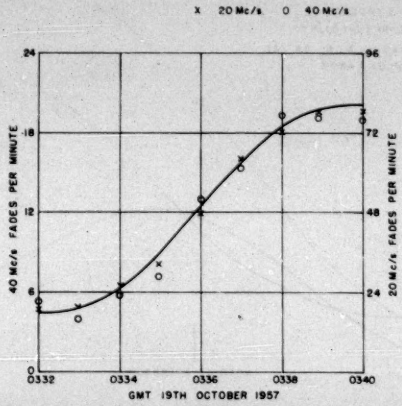

FIG. 7. Observed fading rate due to Faraday rotation. (Reproduced, with permission of the Institution of Electrical Engineers, from B. Burgess, *Proc. Instn. E. E.*, Vol. 105, Part B, p. 113 (1958).)

For Case I, the variation in fading rate will be given by a curve having the same general shape as Curve A of Fig. 6. As far as Case II is concerned it has already been pointed out that the Faraday rotation will be too small to be of practical use.

One possibility exists, at least theoretically, of separating the two ionospheric quantities $\int Ndh$ and N_s, namely, to observe the satellite transmissions simultaneously at two stations separated by a sufficient distance. This method is only applicable when the satellite is observed at a point where dh_s/dt is close to its maximum value, and furthermore, would not be applicable for a circular orbit for which $dh_s/dt = 0$.

V.2
195

The Faraday fading rate observed at stations 1 and 2 can be expressed by

$$\phi_1(t) = k(a_1 \int N dh + b_1 N_s)$$
$$\phi_2(t) = k(a_2 \int N dh + b_2 N_s)$$

where

$$k = 2.36 \times 10^4 f^{-2} \cdot B$$

$$a = \frac{\partial}{\partial t} (\cos\theta \sec\delta)$$

$$b = (dh_s/dt) \cos\theta \sec\delta.$$

Solving these equations leads to

$$N_s = \frac{a_1\phi_2(t) - a_2\phi_1(t)}{k(a_1 b_2 - a_2 b_1)}$$

and

$$\int N dh = \frac{1}{a_1} \left\{ \frac{\phi_1(t)}{k} - b_1 \left[\frac{a_1\phi_2(t) - a_2\phi_1(t)}{k(a_1 b_2 - a_2 b_1)} \right] \right\}.$$

In practice, this method will only be feasible as a means of measuring local electron densities well above the F-layer maximum if the dh_s/dt of the satellite is large throughout the region of interest.

The above discussion applies to the case where the satellite transmissions are received with a fixed, linearly polarized antenna. Another method of utilizing the Faraday effect has been proposed by one of the authors (8). This method is to transmit two closely-spaced frequencies and to receive each signal with a pair of circularly polarized antennas having a continuously variable phase separation, so as to be the equivalent of a continuously rotating dipole. From the time separation of the signal minima on the two frequencies, the integrated electron density may be computed. This method has some advantages, but has the obvious disadvantage of requiring complicated specially designed receiving equipment, whereas the method described in the present paper requires only simple dipole antennas and standard communications receivers.

CONCLUSIONS

The Faraday effect is a very useful tool for the determination of ionospheric parameters that are normally not obtainable by other methods. For the determination of the integrated electron content we may use either lunar radio reflections or transmissions from an artificial satellite. The satellite, however, would have to be placed in an orbit all parts of which lie well above the F region, if the total electron content of the ionosphere is to be determined on a world-wide basis.

The local electron density can be determined from satellite transmissions, but the satellite orbit must extend from below the F-layer peak to well above it, so that dh_r/dt is large throughout the region of interest. In addition, two or more appropriately chosen stations must receive the satellite signals simultaneously to allow separation of the integrated and the local electron densities. Maximum Faraday rotation will be obtained with polar or near-polar orbits, for propagation directions that are not too nearly perpendicular to the Earth's magnetic field, and for frequencies that are low (because of the f^{-2} dependence) but sufficiently above the plasma frequency of the F layer.

Acknowledgment

The authors acknowledge the assistance of Mrs. Mary Tate, who carried out the computations for Figs. 2 to 5, inclusive, on the IBM 650. Mr. Walter Pressman suggested the use of two stations for separation of the effects of local and integrated electron densities.

REFERENCES

(1) K. RAWER, "Die Ionosphäre," Groningen (Holland), P. Noordhoff N. V., 1953, p. 26.
(2) G. H. MUNRO AND R. B. WHITE, *Nature*, Vol. 181, p. 104 (1958).
(3) W. A. S. MURRAY AND J. K. HARGREAVES, *Nature*, Vol. 173, p. 944 (1954).
(4) I. C. BROWNE, J. V. EVANS, J. K. HARGREAVES AND W. A. S. MURRAY, *Proc. Phys. Soc.*, Vol. B69, p. 901 (1956).
(5) J. V. EVANS, *J. Atm. Terr. Phys.*, Vol. 11, p. 250 (1957).
(6) S. J. BAUER AND F. B. DANIELS, *J. Geophys. Res.*, Vol. 63, p. 439 (1958).
(7) B. BURGESS, *Proc. Instn. E. E.*, Part B (London), Vol. 105, p. 113 (1958).
(8) F. B. DANIELS, In "Scientific Uses of Earth Satellites," edited by J. A. VAN ALLEN, Ann Arbor, Univ. of Mich. Press, 1957, pp. 276–282.

V.2
195

ON EXPLANATIONS OF ELECTRIC AND MAGNETIC CONSTANTS AND UNITS

BY

A. T. GRESKY [1]

ABSTRACT

Employing dimensional methods, it is suggested that "explanations" of the free-space dielectric constant ϵ and the magnetic permeability constant μ may lie in their proposed relationships to four highly fundamental quantities; for example, $\epsilon_0 = m_e^3(\hbar\alpha_e c)^{-1}$ and $\mu_0 = \hbar\alpha_e(m_e^2 c)^{-1}$. The latter is considered to reflect a specific intrinsic property of the electron, that is, a constancy in the ratio of its magnetic moment (Bohr magneton) to its spin ($\hbar/2$). The former, equal to $1/\mu_0 c^2$, reflects an additional intrinsic relationship of the electron to light velocity, presumably a characteristic of its associated photons. Other constants and units are similarly analyzed to suggest possible methods for understanding the submicroscopic nature of electric and magnetic phenomena.

INTRODUCTION

The mysteries of interaction-at-a-distance, as encountered in gravitation, electrostatics, magnetostatics, or nuclear binding, are major items of interest to scientific philosophers. The search for general laws of physics and unified field theories inevitably must deal with these mysteries, which scientists usually reconcile or rationalize by use of the mathematical imagination. Explanations of the interaction phenomena are considered to reside in certain unexplainable free-space properties, as exemplified in constants such as G, ϵ, and μ.

Whereas the constant G dealt with forces between particle masses, and thus acquired a knowledgeable value and dimensions of $6.67 \cdot 10^{-8}$ dyne$\cdot$cm$^2\cdot$g^{-2}, the constants ϵ and μ, dealing with forces between abstractions like charges or magnet poles, were necessarily assigned values of dimensionless unity. Proper numerical coefficients and dimensions could then be arbitrarily assigned to units of electrostatic charge (statcoulomb $Q = 1.0\epsilon^{1/2}g^{1/2}cm^{3/2}sec^{-1}$) or magnetostatic poles (maxwell $m = 1.0\ \mu^{1/2}g^{1/2}cm^{3/2}sec^{-1}$) and thus arrive at proper dimensions of unit force (dyne) from defining expressions like $Q_1Q_2(\epsilon r^2)^{-1}$ or $m_1m_2(\mu r^2)^{-1}$.

DISCUSSION

When measurements of the electronic mass m_e and the e/m_e ratios ultimately established that the individual electron's charge e was equal to $4.8 \cdot 10^{-10}$ statcoulomb (and/or that one statcoulomb involved the combined charges of $N_{av} = 2.08 \cdot 10^9$ electrons), there were some investigators who speculated that the electrostatic equation could have

[1] Oak Ridge National Laboratory, Oak Ridge, Tenn.

been alternately written as

$$F = \frac{Q_1 Q_2}{\epsilon r^2} = \frac{(N_a e)_1 (N_a e)_2}{\epsilon r^2} = \frac{(N_a m_e)_1 (N_a m_e)_2}{\epsilon_g r^2} = 1.0 \frac{\text{g cm}}{\text{sec}^2}.$$

Whereas conventionally $\epsilon = 1.0$, it would then be seen that ϵ_g in the last expression, where $r = 1.0$ cm, would necessarily acquire a coefficient and dimensions equal to $3.595 \cdot 10^{-36}$ g sec^{2}cm^{-3}. Noting that ϵ_g^{-1}, equal to $2.77 \cdot 10^{35}$ cm^{3}g^{-1}sec^{-2}, had dimensions identical to $G = 6.67 \cdot 10^{-8}$ cm^{3}g^{-1}sec^{-2}, those who had already recognized the similarity of the equations for electrostatic and gravitational forces, were struck with the possibility that the former as well as the latter dealt with mass interaction-at-a-distance. However, this concept was strongly discouraged by the fact that $(\epsilon_g G)^{-1}$, equal to $4.15 \cdot 10^{42}$, denoted a fantastic deviation from experience in models of gravitational forces.

As suggested in a previous paper (1)[2], if specific physical laws in classical mechanics were granted to be entirely different in nature from the specific laws of electromagnetism or quantum mechanics, the variance of 10^{42} need not be an absolute deterrent to philosophic speculation. When it is recognized that the quantity

$$\epsilon_g = \frac{m_e^2}{\hbar \alpha_e c} = 3.5948 \cdot 10^{-36} \frac{\text{g sec}^2}{\text{cm}^3}$$

(signifying that ϵ_g is peculiarly related to the very fundamental quantities of electronic mass m_e, angular momentum $\hbar$, the fine structure constant α_e, and light velocity c), one might reasonably ask whether the dielectric property of free-space cannot be perspicuously explained in relatively simple terms of mass-space-time; that is, in a similar sense to the "explanation" of gravitational properties by the use of G.

It was shown (1) that G, formulated as $\lambda_0^2 \nu_0^2 M^{-1}$, can be considered as a simple, quantitative, and dimensional statement of the harmonic law of astronomy, indicating a mass-space-time^{-1} relationship of a central massive body to the orbits of its less massive satellites. A new "astronomic" constant $\mu_b = 1.2948 \cdot 10^{-8}$ cm g^{-1}, formulated as $\lambda_a \nu_m (M \nu_r)^{-1}$, was also postulated (1) as a similar modified statement of Blackett's hypothesis (4, 5) which related a solid body's rotational motion to its polar magnetic field intensity. Its dimensions of cm g^{-1}, or cm sec(g sec)$^{-1}$, were indications of yet another quantitative mass-space-time^{-1} law of macroscopic bodies in free-space. Since the magnetic field intensity ν_m could be expressed in sec^{-1} dimensions (gauss $= 1.759 \cdot 10^7$ sec^{-1}) it was possible to visualize and interpret a new dimension of time (or time^{-1}) in the measurement of massive particle properties and mechanics.

[2] Boldface numbers in parentheses refer to the references appended to this paper.

That the gauss unit could be expressed in $\sec^{-1}$ dimensions resulted from a study of "mechanical equivalents" for units and constants employed in electricity, electromagnetism, electrostatics, and magnetostatics. This study revealed, as for ϵ_0 above, that many of these equivalents could be related to m_e, α_e, $\hbar$, c, and numbers (N_{es}, N_{el}, N_{em}) known from em_e^{-1} measurements, for example:

$$\text{specific magnet pole} = \frac{\hbar\alpha_e}{m_e} = 8.44915 \cdot 10^{-3}\ \frac{\text{cm}^2}{\text{sec}},$$

$$\text{maxwell (unit pole)} = \frac{N_{es}\hbar\alpha_e}{m_e} = 1.7594 \cdot 10^{7}\ \frac{\text{cm}^2}{\text{sec}},$$

$$\mu_0 \text{ (of vacuum)} = \frac{\hbar\alpha_e}{m_e^2 c} = 3.0955 \cdot 10^{14}\ \frac{\text{cm}}{\text{g}},$$

$$\text{maxwell} \cdot \text{cm} = \frac{N_{es}\hbar\alpha_e cm}{m_e} = 1.7594 \cdot 10^{7}\ \frac{\text{cm}^3}{\text{sec}},$$

$$\text{Bohr magneton} = \frac{\hbar^2\alpha_e}{2m_e^2 c} = 1.632 \cdot 10^{-13}\ \frac{\text{cm}^3}{\text{sec}},$$

$$\text{gauss} = \frac{N_{es}\hbar\alpha_e}{m_e c m^2} = \frac{1.7594 \cdot 10^{7}}{\text{sec}},$$

$$\text{abamp} = \frac{N_{es} m_e c}{cm} = 5.6837 \cdot 10^{-8}\ \frac{\text{g}}{\text{sec}},$$

$$\text{oersted} = \frac{N_{es} m_e c}{cm^2} = 5.6837 \cdot 10^{-8}\ \frac{\text{g}}{\text{cm sec}},$$

$$\text{statcoulomb} = N_{es} m_e = 1.896 \cdot 10^{-18}\ \text{g},$$

$$\text{abcoulomb} = N_{em} m_e = 5.6837 \cdot 10^{-8}\ \text{g},$$

$$\text{coulomb} = N_{el} m_e = 5.6837 \cdot 10^{-9}\ \text{g, etc.}$$

The observed relationship between μ_0 and the Bohr magneton suggested that the former was a measure of the ratio of an electron's magnetic moment to its spin S_e (or $\hbar/2$) and that the

$$\text{Bohr magneton} = \mu_0 S_e = \frac{\hbar S_e \alpha_e}{m_e^2 c} = 1.632 \cdot 10^{-13}\ \frac{\text{cm}^3}{\text{sec}}.$$

Since several investigators (2–5) have considered that the magnetic field intensities of both macroscopic and submicroscopic particles are proportional to their mass and angular momentum, it was finally considered that

$$L_m = m_e\mu_g = \frac{\hbar\alpha_e}{m_e c} = 2.8185\cdot 10^{-13}\text{ cm},$$

sometimes (6) called the electron's classical radius, might actually be a universal constant of submicroscopic particle physics relating mass ·magnetic moment to particle spin. This indicated the possibility that yet another quantity $M_e = m_e\alpha_e^{-1}$, evident in L_m, was also a universal constant relating any submicroscopic particle's mass to its fine structure constant. It was thus conceived that α_e is a specific electronic quantity which might define a constancy in the relationship of the electron's magnetic field intensity ν_m to its angular velocity ν_r (for example, as surmised from $\nu_r = E_e\hbar^{-1}$), that is,

$$\alpha_e = \frac{m_e}{M_e} = \left(\frac{\nu_m}{\nu_r}\right)_e = 7.2978\cdot 10^{-3}.$$

Another quantity, $F_g = G\mu_b^{-2} = 3.9782\cdot 10^{8}$ g cm sec^{-2}, relating μ_b to the gravitational constant G, was considered (1) to be a general constant of physics, since, also,

$$F_g = \frac{M_e^3c^2}{\hbar} = \frac{\hbar c}{L_m^2} = \frac{M_e c^2}{L_m} = 3.9782\cdot 10^{8}\,\frac{\text{g cm}}{\text{sec}^2},$$

suggesting the existence of a single "law" of quantum mechanics, electromagnetism, and classical mechanics. (It has been noted (7) in the press that Dr. Werner Heisenberg's unified field equation might depend importantly on three constants: that is, $\hbar$, c, and an unknown constant x, with dimensions of length approximating the 10^{-13} cm range of nuclear forces. Since the above quantity $L_m = 2.8185\cdot 10^{-13}$ cm has properties suggestive of the constant x, and since $\hbar$ and c also appear in quantity F_g, one may speculate whether the latter is an essential or component part of Dr. Heisenberg's hypothesis of the unified field.) Returning to the "explanation" of the dielectric constant ϵ_g and the magnetic permeability constant μ_g, it is of interest to note also that

$$\epsilon_g = \frac{m_e m_e}{L_m m_e c^2} = \frac{m_e}{L_m c^2} = 3.5948\cdot 10^{-36}\,\frac{\text{g sec}^2}{\text{cm}^3},$$

$$\mu_g = \frac{L_m}{m_e} = 3.0955\cdot 10^{14}\,\frac{\text{cm}}{\text{g}},\text{ and}$$

$$F_g = \frac{\hbar c}{m_e^2\mu_g^2} = \frac{\hbar c^3\epsilon_g}{m_e^2\mu_g} = \frac{\hbar c^5\epsilon_g^2}{m_e^2} = 3.9782\cdot 10^{8}\,\frac{\text{g cm}}{\text{sec}^2}.$$

With knowledge of L_m's meaning, it may then be surmized that ϵ_g reflects a fundamental relationship between the electron's magnetic mo-

ment, spin, and light velocity (presumably associated with a characteristic photon of rest mass m_* with energy m_*c^2 equal m_*v^2). Similarly, μ_g would appear to reflect a fundamental relationship between the electron's magnetic moment and its spin. The general constant F_g may then be shown to relate an electron's energy $E_*(m_*v^2$ or $m_*c^2)$, a wave-"radius" λ_0 (characteristic of its energy, according to $\hbar cE_*^{-1}$), its mass m_*, its magnetic moment M_b, and its spin S_*; that is,

$$F_g = \frac{E_*\lambda_0 S_*^2}{m_*^2 M_b^2} = \frac{\text{energy}\cdot\text{wave-radius}\cdot\text{spin}^2}{\text{mass}^2\cdot\text{magnetic moment}^2} = 3.9782\cdot 10^8\,\frac{\text{g cm}}{\text{sec}^2}.$$

The several interrelationships observed among (1) the general constants $\hbar$, c, M_*, L_m, F_g, (2) the electronic constants m_*, α_*, S_*, M_b, μ_g, and ϵ_g, and (3) the numbers N_{*0}, N_{*m}, and N_{*l}, may possibly afford clues to "explanations" of all electric and magnetic phenomena. A suggested approach to the use of such clues is outlined in the Appendix. Although the highly developed technology of electronics and magnetism has not required actual explanations of space properties such as ϵ, μ, or resistivity, it may be that electromagnetic science and theory would profit from any possible resolution of their mysteries.

Acknowledgment

The writer acknowledges, with sincere thanks, the encouragement and constructive criticism of Floyd L. Culler, Director of the Chemical Technology Division of Oak Ridge National Laboratory. The helpful suggestions and friendly review of this paper by Dr. Stan H. Jury, Professor of Chemical Engineering, University of Tennessee, and Dr. B. A. Soldano, member of the Chemistry Division of ORNL, are also gratefully acknowledged. In memory of an esteemed friend and critic, the writer also wishes to express his gratitude to Dr. J. M. Dalla Valle, deceased, of the Georgia Institute of Technology.

REFERENCES

(1) A. T. GRESKY, "New Physical Constants from Dimensional Analysis," JOUR. FRANKLIN INST., Vol. 265, p. 85 (1958).
(2) H. A. WILSON, "An Experiment on the Origin of the Earth's Magnetic Field," *Proc. Roy. Soc.*, Vol. 104, p. 451 (1923).
(3) W. F. G. SWANN, "A Generalization of Electrodynamics," *Phil. Mag.*, Vol. 3, p. 1088 (1927).
(4) J. FUCHS, "Blackett's Hypothesis of the Magnetic Field of Rotating Bodies," *Nature*, Vol. 161, p. 599 (1948).
(5) T. GOLD, "Rotational and Terrestrial Magnetism," *Nature*, Vol. 163, p. 513 (1949).
(6) G. GAMOW, "Structure of Atomic Nuclei and Nuclear Transformations," Oxford, Clarendon Press, 1937, pp. 1, 5.
(7) HARRY GILROY, "A Basic Equation for Matter Given," in *The New York Times*, April 26, 1958, p. 2.

APPENDIX

Hypothetical Models of Electron Mechanics and Magnetism

Quantities (1) through (8) in Table I may be suggested to describe the rotating electron at three different energies and/or voltages (abvolt, volt, and 300 volts); that is, characteristic of potential differences or electromotive forces encountered in the unit systems of electromag-

TABLE I.—*Mass, Space, and Time*$^{-1}$ *Properties of Electrons at 10*$^{-8}$, *1.0, and 300 Ev*

	10^{-8}Ev Electron (Emu System)	1.0Ev* Electron (Pract. Elect.)	300Ev Electron (Esu System)
(1) m_e = electron rest mass$_e$ =	$9.11\cdot10^{-28}$	$9.11\cdot10^{-28}$	$9.11\cdot10^{-28}$ g
(2) $\lambda_e = \hbar(2m_ec)^{-1} = S_e(m_ec)^{-1}$ =	$1.93\cdot10^{-11}$	$1.93\cdot10^{-11}$	$1.93\cdot10^{-11}$ cm
(3) $\lambda_r = (\hbar^2/m_eE_e)^{1/3}$ =	$2.76\cdot10^{-4}$	$2.76\cdot10^{-6}$	$1.59\cdot10^{-9}$ cm
(4) $\nu_r = E_e\hbar^{-1}$ =	$1.52\cdot10^{7}$	$1.52\cdot10^{15}$	$4.56\cdot10^{17}$ sec^{-1}
(5) $\nu_m = E_e\alpha_e\hbar^{-1}$ =	$1.11\cdot10^{5}$	$1.11\cdot10^{13}$	$3.32\cdot10^{15}$ sec^{-1}
(6) $\nu_0 = E_e\hbar^{-1} = E_e\hbar^{-1}$	$1.52\cdot10^{7}$	$1.52\cdot10^{15}$	$4.56\cdot10^{17}$ sec^{-1}
(7) $\lambda_0 = \hbar cE_e^{-1}$ =	$1.97\cdot10^{3}$	$1.97\cdot10^{-5}$	$6.58\cdot10^{-8}$ cm
(8) $m_e = E_ec^{-2}$ =	$1.78\cdot10^{-41}$	$1.78\cdot10^{-33}$	$5.35\cdot10^{-31}$ g
(9) $m_e\lambda_r^2\nu_r^2 = E_e$ =	$1.60\cdot10^{-20}$	$1.60\cdot10^{-12}$*	$4.80\cdot10^{-10}$ g cm^{2}sec^{-2}
(10) $m_e\lambda_0^2\nu_0^2 = E_e$ =	$1.60\cdot10^{-20}$	$1.60\cdot10^{-12}$*	$4.80\cdot10^{-10}$ g cm^{2}sec^{-2}
(11) $\lambda_0\nu_0 = c$ =	$3.00\cdot10^{10}$	$3.00\cdot10^{10}$	$3.00\cdot10^{10}$ cm sec^{-1}
(12) $m_e\lambda_0^2\nu_0 = m_e\lambda_r^2\nu_r = \hbar$ =	$1.05\cdot10^{-27}$	$1.05\cdot10^{-27}$	$1.05\cdot10^{-27}$ g cm^{2}sec^{-1}
(13) $m_e\lambda_ec = \hbar/2 = S_e$ =	$5.27\cdot10^{-28}$	$5.27\cdot10^{-28}$	$5.27\cdot10^{-28}$ g cm^{2}sec^{-1}
(14) $\lambda_r^2\nu_r = \hbar/m_e^{-1}$ =	$1.16\cdot10^{9}$	$1.16\cdot10^{9}$	$1.16\cdot10^{9}$ cm^{2}sec^{-1}
(15) $\lambda_r^2\nu_m = \hbar\alpha_em_e^{-1} = L_mc$	$8.45\cdot10^{-3}$	$8.45\cdot10^{-3}$	$8.45\cdot10^{-3}$ cm^{2}sec^{-1}
(16) $\lambda_r^2\nu_m(\lambda_0\nu_0)^{-1} = m_eM_bS_e^{-1} = L_m$	$2.82\cdot10^{-13}$	$2.82\cdot10^{-13}$	$2.82\cdot10^{-13}$ cm
(17) $\lambda_r^2\lambda_e = \lambda_r^4(2\lambda_0)^{-1}$ =	$2.94\cdot10^{-15}$	$2.94\cdot10^{-25}$	$9.77\cdot10^{-29}$ cm^3
(18) $\lambda_r^2\lambda_e\nu_m = M_b$	$1.63\cdot10^{-13}$	$1.63\cdot10^{-13}$	$1.63\cdot10^{-13}$ cm^{3}sec^{-1}
(19) $\nu_m\nu_r^{-1} = \alpha_e$ =	$7.29\cdot10^{-3}$	$7.29\cdot10^{-3}$	$7.29\cdot10^{-3}$
(20) $m_e\lambda_0^2\nu_m^2/2 = E_{Ryd.}$ =	$2.18\cdot10^{-11}$	$2.18\cdot10^{-11}$	$2.18\cdot10^{-11}$ g cm^{2}sec^{-2}
(21) $\lambda_r^2\nu_m(m_e\lambda_0\nu_0)^{-1} = \mu_g$ =	$3.09\cdot10^{14}$	$3.09\cdot10^{14}$	$3.09\cdot10^{14}$ cm g^{-1}
(22) $m_e(\lambda_r^2\nu_m\lambda_0\nu_0)^{-1} = \epsilon_g$ =	$3.59\cdot10^{-26}$	$3.59\cdot10^{-26}$	$3.59\cdot10^{-26}$ g sec^{2}cm^{-3}
(23) N = no. of electrons.	$6.24\cdot10^{19}$	$6.24\cdot10^{19}$	$2.08\cdot10^{9}$
(24) $NE_e = NE_e = E_t$ =	$1.00\cdot10^{9}$	$1.00\cdot10^{7}$	$1.00\cdot10^{9}$ g cm^{2}sec^{-2}
(25) $\lambda_r^2\nu_r^2 = E_em_e^{-1} = V_g$ =	$1.76\cdot10^{7}$	$1.76\cdot10^{15}$	$5.27\cdot10^{17}$ cm^{2}sec^{-2}

* One electron-volt, equal to $1.6\cdot10^{-12}$ erg.

netism, practical electricity, and electrostatics. The rest mass m_e is considered to be located in a dense spherical "nucleus" of λ_e radius, shown as constant for all energies E_e. Note that $4\pi\lambda_e$ would be equal to the Compton wave-length $\lambda = h/m_ec$, and that λ_e is equal to $\hbar/2$ (half-integral "spin") divided by m_ec, suggesting a relationship of "spin" to m_e's original creation near light velocity. The "equatorial" or effective radius λ_r, shown to increase with decreasing energy, will be noted as equal to the de Broglie wave-length, $\lambda = h/m\nu$, divided by 2π. Quantity (17) suggests that m_e's effective volume, dependent on the product of λ_e (axial radius) and λ_r^2, becomes increasingly oblate with decreasing energy. The value for ν_r (angular velocity, in radians·sec^{-1}) will be observed as 2π times greater than the wave-frequency ν, equal to $E_e\hbar^{-1}$, which would characterize the given electron as a wave of radiation. Quantity (8) suggests that characteristic photons of rest mass m_e, with energy E_e equal E_e, become associated with electrons at all energies. (Note that $m_e + m_e$ does not become appreciably greater than m_e until the energy approaches m_ec^2, at which point $m_e + m_e$ would approach $2m_e$.) The photon of rest mass m_e may be imagined as a rotating "particle" or standing-wave with angular velocity ν_0 equal to m_e's angular velocity ν_r and a radius λ_0 equal to $c\nu_0^{-1}$ or $\hbar cE_e^{-1}$. (It may also be imagined as revolving about m_e in an orbit of radius λ_0 with angular velocity ν_0, exhibiting a

peripheral velocity $\lambda_0\nu_0$ equal to c. If emitted as radiation, it would appear as a light particle-wave of frequency $\nu_0(2\pi)^{-1}$ and length $2\pi\lambda_0$.) Finally, m_s may be considered to possess a magnetic field, polarized along axis λ_s and perpendicular to the equatorial plane λ_r^2, having an intensity ν_m equal to $\nu_r\alpha_s$ vibrations (?) per second. The measure of this field, in gauss, for the three given electrons may be found by dividing the ν_m values by $1.759\cdot10^7$ sec^{-1} gauss^{-1}. Note, from quantities (15) and (18), that each free electron may then be characterized as a magnetic pole equal to $4.8\cdot10^{-10}$ maxwell and as having magnetic moment of $9.3\cdot10^{-21}$ maxwell·cm, or one Bohr magneton (where, as previously (1) suggested, the maxwell and the Bohr magneton are equivalent to $1.759\cdot10^7$ $\text{cm}^3\text{sec}^{-1}$ and $1.63\cdot10^{-13}$ $\text{cm}^3\text{sec}^{-1}$, respectively).

By formulation, quantities (12) and (13) suggest the similarities that exist in the constants of angular momentum $\hbar$ and spin S_s. Quantities (19) through (22) suggest the formulation of electronic constants such as the fine structure constant, the Rydberg energy, and the magnetic permeability and dielectric constants of free-space. Note that quantity (16), sometimes (6) referred to as the "classical electron radius," may appear to be a universal constant relating the mass, magnetic moments, and spins of electrons (and perhaps of other submicroscopic particles).

Quantity (23) may be determined from knowledge of charge-to-mass ratios, and quantity (24) defines the energy units (erg and joule) in the cgs systems of measurement. Quantity (25) suggests the numerical and dimensional values of mechanical equivalents for the familiar abvolt, volt, and statvolt of potential difference or electromotive force.

Suggested Definitions of Units and Constants of Electricity and Magnetism

An understanding of electron properties as shown in (1) through (8) above, as well as certain interrelationships as suggested in (9) through (25), may be helpful in interpreting the fundamental implications of the suggested (1) mechanical equivalents. For example, where

$N_{ss} = 2.0823\cdot10^9$,	$m_s = 9.1055\cdot10^{-28}$ g,
$N_{sm} = 6.242\cdot10^{15}$,	$\alpha_s = 7.2978\cdot10^{-3}$,
$N_0 = 1.0$,	$\hbar = 1.0542\cdot10^{-27}$ g $\text{cm}^2\text{sec}^{-1}$,
$r = 1.0$ cm,	$c = 2.9977\cdot10^{10}$ cm sec^{-1},
$l = 1.0$ cm,	$M_s = m_s\alpha_s^{-1} = 1.2477\cdot10^{-25}$ g
$a = 1.0$ cm,	$L_m = \hbar\alpha_s(m_sc)^{-1} = 2.8185\cdot10^{-13}$ cm,
$v = rt^{-1} = 1.0$ cm sec^{-1},	$t = 1.0$ sec,

and where r, a, and l represent mutually perpendicular directions of separation or length, one may alternately derive equivalents for quantities employed in electrostatics, magnetostatics, and electromagnetism, as shown below.

Electrostatic Quantities

$$\frac{Q_{ss}^-Q_{ss}^+}{r^2}\times\frac{1.0}{g}=F_{ss};\quad\frac{(N_{ss}m_s^-)(N_{ss}m_s^+)}{cm^2}\times\frac{\hbar\alpha_sc}{N_0m_s^2}=\frac{N_{ss}^2}{N_0cm^2}\hbar\alpha_sc \tag{26}$$

suggests an equivalent of $1.896\cdot10^{-18}$ g for the statcoulomb, 1.0 g cm sec^{-2} for the dyne of electrostatic force, and $3.5948\cdot10^{-36}$ g $\text{sec}^2\text{cm}^{-3}$ for the dielectric constant of free-space. Note, in this case, that Q_{ss}^- refers to a number of free electron masses, while Q_{ss}^+ may refer to a similar number of positrons (of rest mass m_s) located near the nuclei of ionized atoms. Note that ϵ_g might also have been written as $N_0m_sM_s(\hbar c)^{-1}$ or $N_0m_s(L_mc^2)^{-1}$, and that dielectric values greater than ϵ_g (vac.) would suggest an increase in the number N_0. Note that an equivalent unit of potential energy or work would be equal to $F_{ss}r$ or one erg, and a unit of surface charge density might be written as $Q_{ss}(al)^{-1}$, or $N_{ss}m_scm^{-2}$, or $1.896\cdot10^{-18}$ g cm^{-2}. The unit of electric field intensity A_g might be written, as follows:

$$\frac{Q_{ss}^+}{r^2}\times\frac{1}{\epsilon_g}=A_g;\quad\frac{N_{ss}m_s^+}{cm^2}\times\frac{L_mc^2}{N_0m_s}=\frac{N_{ss}}{N_0cm^2}L_mc^2, \tag{27}$$

suggesting an equivalent of $5.2742 \cdot 10^{17}$ cm sec^{-2} (dimensions of acceleration) for the statvolt·cm^{-1}. The unit of potential difference V_e, the statvolt, would be equal to $A_e r$ or $5.2742 \cdot 10^{17}$ cm^{2}sec^{-2}, and the unit of capacitance C_e would be equal to

$$Q_{ss} \times \frac{1}{V_e} = C_e; \quad N_{ss} m_s \times \frac{N_0 cm}{N_{ss} L_m c^2} = \frac{N_0 m_s cm}{L_m c^2} \tag{28}$$

suggesting an equivalent of $3.5948 \cdot 10^{-36}$ g sec^{2}cm^{-2} for the statfarad unit.

Magnetostatic Quantities

$$\frac{m_g^- m_g^+}{a^2} \times \frac{1}{\mu_g} = F_{ms}; \quad \frac{(N_{ss} L_m c)^- (N_{ss} L_m c)^+}{cm^2} \times \frac{m_s}{N_0 L_m} = \left(\frac{N^2_{ss} m_s}{N_0 cm^2}\right) L_m c^2 \tag{29}$$

suggests an equivalent of $1.7594 \cdot 10^7$ cm^{3}sec^{-1} for the unit magnetic pole or maxwell, $3.0955 \cdot 10^{14}$ cm g^{-1} for the magnetic permeability constant μ_g of free-space, and 1.0 g cm sec^{-2} for the dyne of magnetostatic force. Note that the distance of pole separation is symbolized by a rather than r as in the electrostatic case, and that the unit of magnetic field intensity B_g would be written as

$$\frac{m_g}{rl} = B_g; \quad \frac{N_{ss} L_m c}{rl} = \frac{N_{ss} L_m c}{cm^2}, \tag{30}$$

suggesting an equivalent of $1.7597 \cdot 10^7$ sec^{-1} for the gauss, or maxwell-per-unit-area. Note that μ_g might also be written as $N_0 h \alpha_s (m_s{}^2 c)^{-1}$, and that it is equal to $1/e_g c^2$. Also note, for permeabilities greater than μ_g (vac.), that an increase in the number N_0 would be indicated. The maxwell·cm of magnetic moment M_g could be written as

$$m_g a = B_g arl = M_g = N_{ss} L_m ca \tag{31}$$

suggesting an equivalent of $1.7594 \cdot 10^7$ cm^{3}sec^{-1}, equal to $1.08 \cdot 10^{20}$ Bohr magnetons.

Electromagnetic Quantities

$$B_g vl = \frac{m_g}{rl} \times \frac{r}{l} \times l = V_g; \quad \frac{N_{ss} L_m c}{cm^2} \times \frac{\text{cm}^3}{sec} = \frac{N_{ss} L_m c}{sec}$$

suggests an equivalent of $1.7594 \cdot 10^7$ cm^{2}sec^{-2} for the abvolt unit of electromotive force. Note the symbolic indication that such a force is produced along the length l of a wire moving with velocity rt^{-1} (in the r direction and perpendicular to magnetic lines of force oriented in an a direction). The equivalent for the abvolt·cm^{-1} unit of electric field intensity A_g along l would be $V_g l^{-1}$ or $1.7594 \cdot 10^7$ cm sec^{-2}.

$$B_g = \mu_g H_g; \quad \frac{N_{ss} L_m c}{r^2} = \frac{N_0 L_m}{m_s} \times \frac{N_{ss} m_s c}{N_0 r^2} \tag{32}$$

suggests an equivalent of $5.6837 \cdot 10^{-8}$ g cm^{-1} sec^{-1} for the oersted unit of magnetizing force H_g, where a unit current

$$I_g = \frac{H_g r^2}{l}; \quad \frac{N_{ss} m_s c}{Nl} = \frac{N_{ss} m_s c}{N_0 r^2} \times \frac{r^2}{l} \tag{33}$$

equivalent to $5.6837 \cdot 10^{-8}$ g sec^{-1} or one abamp, flowing in a conductor arc of length l, produces a field of gauss intensity at radius r, in a medium of permeability μ_g. Note that I_g can also be written as $N_{sm} m_s \text{sec}^{-1}$. From

$$V_g = R_g I_g; \quad \frac{N_{ss} L_m c}{sec} = \frac{N_{ss} L_m c}{N_{sm} m_s} \times \frac{N_{sm} m_s}{sec} \tag{34}$$

an equivalent for the abohm of resistance R_g would be equal to $3.0955 \cdot 10^{14}$ cm^2 g^{-1}sec^{-1}. Note that the abohm·cm of resistivity R_G might then be written as $N_{ss} L_m c l^{-1} / N_{sm} m_s (ar)^{-1}$ or $3.0955 \cdot 10^{14}$ cm^{3}g^{-1}sec^{-1}, implying that it measures an empirical ratio of electron magnet poles per

unit length to electrons per unit area of the conductor. Electromagnetic force F_{ee} between two parallel current-carrying wires, *in vacuo*, can be expressed as

$$\frac{(I_e l)_1 (I_e l)_2}{r^2} \times \mu_0 = F_{ee}; \quad \frac{N_{ee}^2 m_e^2 c^2 l^2}{N_0^2 l^2 r^2} \times \frac{N_0 \hbar a_e}{m_e^2 c} = \frac{N_{ee}^2 \hbar a_e c}{N_0 r^2}. \tag{35}$$

The dyne unit of electrical force F_{el} can be expressed as

$$\frac{V_e I_e l}{l} = F_{el}; \quad \frac{N_{ee} L_m c}{l \text{ sec}} \times \frac{N_{em} m_e}{\text{sec}} \times \text{sec} = \left(\frac{N_{ee} N_{em} m_e}{\text{cm sec}} \right) L_m c.$$

Interpretations from Mechanical Equivalences

From examples in the above discussions, and the data in Table I, it is possible to evolve certain imaginative interpretations of phenomena. One example may be considered, as follows. From quantities (2), (3), (15), (29), (30), and (31), one might surmise that: (*a*) a magnetic pole face of area rl, with gauss intensity, is characterized by $2.0823 \cdot 10^9$ polarized electrons (and/or electron magnet poles $\lambda_r^2 \nu_m$) per unit area, with their equatorial λ_r^2 planes parallel to the face; (*b*) since each electron would thus occupy a maximum of $4.8 \cdot 10^{-10}$ cm^2, its, minimum allowed energy might appear to be in the order of 10^{-17} g cm^{2}sec^{-2} or $6.25 \cdot 10^{-6}$ ev that is, where its λ_r would not exceed about 10^{-8} cm; (*c*) if the magnet were a cube with 1.0-cm sides with a magnetic moment of one maxwell·cm, the foregoing would imply that cm·λ_e^{-1} or $5.18 \cdot 10^{10}$ electron poles along the magnet's length a would be required to account for $1.08 \cdot 10^{20}$ Bohr magnetons within the cube. Thus, one might visualize a magnetic field of gauss intensity as containing $2.082 \cdot 10^9$ parallel "lines" of electrons per cm^2 of rl area. The individual lines, polarized along direction a and perpendicular to rl would then appear to consist of some $5.18 \cdot 10^{10}$ axially-connected electrons per cm of line-length. A 1000-gauss field might thus be characterized by $2.082 \cdot 10^{12}$ such "lines" per cm^2 of field area.

Similarly, from (34) and its discussion, a cubic conductor with 1.0-cm sides, having a hypothetical resistivity of 1.0 abohm·cm (probably characteristic of supra-conductors), might be visualized to contain $6.242 \cdot 10^{19}$ electrons per cm^2 of face area ar, oriented with their λ_r^2 planes perpendicular to the face; $2.082 \cdot 10^9$ electron lines, with their axes perpendicular to the direction of current flow, would then be located along length l. (Note that good metal conductors have resistivities in the order of 1.0 microhm·cm, or 10^3 abohm·cm, indicating a less favorable, or higher, ratio than $N_{ee} N_{em}^{-1}$.)

From (35), concerning the fields and forces of two current-carrying wires *in vacuo*, an example of oppositely directed currents provides a mechanical concept of geometrical and polar relations among the three fields involved in simultaneous electrical, electromagnetic, and dielectric forces. The two electric fields in opposite directions l contribute to the induction of a magnetic field in the space between them, oriented in direction a. The magnetic fields circling each wire can be visualized as lines of axially-connected electrons, with line-density increasing near the wires, and being enhanced in the region between the wires. Relative polarization in the latter region would be such as to suggest magnetic dipolar repulsion of the lines, and thus a mechanical force on the wires. A dielectric field (perpendicular to both the electric and magnetic field directions) also exists in the r direction between the wires, however its energy would depend on $V_e^3 C_e$ and would become significant only at higher voltages.

Relating Constants and Units to the Universal Constant F_e

Since each of the various constants mentioned in the above discussions is related to m_e, c, α_e, and/or $\hbar$, it will be noted that each can be related to the other by use of a general equation exemplified below:

$$F_e = \frac{m_e^3 c^3}{\alpha_e^2 \hbar} = \frac{c^3}{\mu_e \alpha_e} = \frac{e_e c^4}{\alpha_e} = \frac{\hbar c^3}{2 M_B \alpha_e} = \frac{2 E_R m_e c}{\hbar \alpha_e^4} = \frac{m_e^3 c^3}{2 S_e \alpha_e^3} = \frac{S_e c^3}{M_\mu \alpha_e}$$

$$= \frac{M_e c^3}{\hbar} = \frac{m_e c^2}{L_m \alpha_e} = 3.9782 \cdot 10 \ \frac{\text{g cm}}{\text{sec}^2}.$$

It will also be recognized that certain interrelationships of the various units and constants will also be equal to F_g, for example:

$$F_g = \frac{R_g I_g \lambda_g H_g}{m_e \mu_g B} = \frac{(\text{abohm})(\text{abamp})(\lambda_g)_{em}(\text{oersted})}{(\text{electronic mass}_e)(\mu_g)(\text{gauss})} = 3.9782 \cdot 10^8 \frac{\text{g m}}{\text{sec}^2}$$

$$F_g = \frac{R_g P \lambda_g Q_{es}^2}{m_e m_g^2} = \frac{(\text{abohm})(\text{abwatt})(\lambda_g)_{em}(\text{statcoulomb})^2}{(m_e)_{em}(\text{maxwell})^2} = 3.9782 \cdot 10^8 \frac{\text{g cm}}{\text{sec}^2}$$

$$F_g = \frac{I_g R_G F_{em} \lambda_g e_g}{Q_{em} m_e \mu_g} = \frac{(\text{abamp})(\text{abohm} \cdot \text{cm})(\text{dyne})(\lambda_g)_{em}(e_g)}{(\text{abcoulomb})(m_e)_{em}(\mu_g)} = 3.9782 \cdot 10^8 \frac{\text{g cm}}{\text{sec}^2}.$$

It will be noted that the latter expression contains a relationship among the three elusive properties of space (or media), that is, resistivity (R_G), dielectric (e_g), and magnetic permeability (μ_g). Speculatively, it may be hoped that such knowledgable relationships can eventually lead to a clearer perception into the nature of medial properties and the three related forces (electric, electromagnetic and electrostatic) which characterize electron motions and interactions.

V.2(
195

THE INFLUENCE OF GRAVITY ON THE FOLDING OF A LAYERED VISCOELASTIC MEDIUM UNDER COMPRESSION

BY

M. A. BIOT [1]

ABSTRACT

The theory of folding of a layered viscoelastic medium under a horizontal compression parallel with the layer, as developed in previous publications (1, 2, 3),[2] is extended to take into account the influence of gravity. Characteristic features of the folding are evaluated in terms of nondimensional parameters. The influence of gravity appears through a parameter which depends on the relative magnitude of the gravity forces and the horizontal compression. Specific cases discussed are that of a layer on top of a half-space and the layer embedded between two half-spaces, with the bottom medium either denser or less dense than the top one.

1. INTRODUCTION

In references 1 and 2 we have investigated the folding due to instability when a layered viscoelastic medium is subject to a compression in a direction parallel with the layer. The layer was assumed to be embedded in an indefinite solid or lying on the surface of a half-space. The problem was analyzed from a very general viewpoint and the viscoelastic and hereditary characteristics of the material were assumed to obey the most general linear laws. In particular, conclusions are drawn for materials which obey the Onsager relations and the laws of the thermodynamics of irreversible processes as formulated in some our previous work (7, 8). The folding was also evaluated for various specific combinations of viscoelastic media, and attention was given to the effect of interfacial friction at the boundary and to the evaluation of the magnitude of the folding as distinct from mere instability (2). In the cited work we used an approximation of the "plate theory" type to represent the folding of the layer. In reference 3 this approximation was discarded and the problem was treated by using exact equations of the stability of a prestressed continuum as developed in earlier papers (4, 5, 6, 7). The problem of stability of the surface of a viscoelastic half-space was also treated as a particular case.

In the present analysis we are dealing with the problem of folding of a layer, either lying on top of a viscoelastic half-space, or embedded between two such half-spaces. When in addition to a compression parallel with the direction of the layer there is also a uniform gravity field perpendicular to this direction, we are therefore dealing with in-

[1] Consultant, Shell Development Company, Houston, Texas.

[2] The boldface numbers in parentheses refer to the references appended to this paper.

stability under a combined state of prestress—the horizontal compression in the layer, and a prestress due to gravity which is assumed to be a hydrostatic field. The addition of gravity to the problem is essential of course if we have in mind some of the geological applications. We shall discuss these at a later date.

A general formulation of the problem is outlined in Section 2. From the previously established theory (**4, 5, 6, 7**), we derive the equations for the stability problem of a continuum under a uniform compression and a hydrostatic stress gradient due to gravity. These equations are quite general and may be applied to both compressible and incompressible media. For simplicity we have applied the theory only to incompressible media and in Section 3 we show that in this case simplifications may be introduced along with a "plate type" equation for the layer. This leads to a very simple equation for the folding of a layer lying on top of a half-space. The case of a layer and underlying medium which are incompressible and purely viscous is discussed in Section 4. The dominant wave length (that is, that whose amplitude grows at the fastest rate) is evaluated as a function of the ratio of the viscosity coefficients of the two media and a nondimensional parameter which represents the influence of gravity. This parameter is a ratio of two quantities, one is the pressure of a column of underlying material of height equal to the layer thickness and the other the compressive horizontal force. The density of the layer itself does not enter into the picture because of our assumption that the layer behaves like a thin plate of constant thickness. The relative amplitude of the folding for the dominant wave length is also evaluated. This yields an indication of the magnitude of the instability.

Section 5 discusses the case of a layer embedded between two different materials. The materials are again assumed incompressible and purely viscous. Two cases must be considered. In the first case the underlying material is denser and the effect of gravity is stabilizing. The theory is the same as for the layer lying on top of the half-space except for modified parameters which introduce the sum of the viscosities of top and bottom media and the difference of their densities. The effect of gravity tends to shorten the dominant wave length. The second case is that of an inverse density gradient, that is, the underlying material is lighter than the top one. The layer is then unstable because of gravity alone. The phenomenon then becomes somewhat more complex. For certain ranges of the parameters the combined effect of gravity and compression will increase the dominant wave length while in another range the dominant wave length will be controlled by geometric factors such as the depth of the surrounding medium. It should be kept in mind that we have not taken into consideration any inertia forces. The deformations are therefore assumed to be sufficiently slow for these forces to be negligible.

Strictly speaking, the theory is also restricted to infinitesimal deformations but in practice it is of course applicable to a large category of observable phenomena in the same sense as this is understood to be true in the applications of the classical linear Theory of Elasticity. Furthermore it is most likely that the folding wave length which appears in the incipient phase of the instability will also correspond to the characteristic feature in the later phases with large deformations. An experimental program of model tests on the folding of layered viscoelastic media has been initiated. Results are in good agreement with the theory. They will be presented in later publications.

2. GENERAL EQUATIONS FOR THE DEFORMATION OF A PRESTRESSED MEDIUM

In reference 3 we have analyzed the folding instability under compression of a layered viscoelastic medium by using the exact equations for the deformation of an anelastic continuum under prestress. These equations are the same as those which we established in references 4, 5 and 6 for the elastic continuum. The general applicability of these equations to anelastic media was discussed in reference 7. A brief rederivation of the equations was also presented in reference 3. In the previous work we did not introduce the gravity force. In the following we shall consider the prestress to result from both the lateral compressive forces on the layered material and the hydrostatic pressure gradient due to its weight. In the present section we shall write out the equations and boundary conditions for this particular state of prestress. We shall also restrict ourselves to two-dimensional deformations. As established in the work quoted above the incremental stress field of the continuum satisfies the equations

$$\frac{\partial s_{11}}{\partial x} + \frac{\partial s_{22}}{\partial y} + \rho Y\omega - 2S_{12}\frac{\partial \omega}{\partial x} + (S_{11} - S_{22})\frac{\partial \omega}{\partial y} + \frac{\partial S_{11}}{\partial x} e_{yy} - \left(\frac{\partial S_{11}}{\partial y} + \frac{\partial S_{12}}{\partial x}\right) e_{xy} + \frac{\partial S_{12}}{\partial y} e_{xx} = 0 \quad (1)$$

and another similar equation obtained by permuting x and y, 1 and 2 and changing ω into $-\omega$. The coordinate system is assumed to be clockwise. In these equations S_{11}, S_{22}, S_{12} are the initial stress components in the x, y plane, s_{11}, s_{22}, s_{12} are the incremental stresses, and ρY is the y component of the body force per unit volume (ρ mass density). The displacement field u, v yields the strain components

$$e_{xx} = \frac{\partial u}{\partial x} \qquad e_{yy} = \frac{\partial v}{\partial y} \quad (2)$$

$$e_{xy} = \frac{1}{2}\left(\frac{\partial v}{\partial x} + \frac{\partial u}{\partial y}\right)$$

and the rotation

$$\omega = \frac{1}{2}\left(\frac{\partial v}{\partial x} - \frac{\partial u}{\partial y}\right). \tag{3}$$

In this representation the stress components s_{ij} are the incremental stresses at the displaced point $x + u$, $y + v$, and relative to axes rotated by an angle ω. The strain components e_{ij} are also referred to the same displaced and rotated axes. The latter are of course not distinct, in the first order, from the classical components for small strain.

Consider now a particular case of prestress, namely a combination of a horizontal compressive stress P and a hydrostatic stress due to gravity. The gravity force is assumed parallel with the y axis. In that case

$$Y = g \tag{4}$$

where g is acceleration of gravity and the initial state of stress is

$$\begin{aligned} S_{11} &= -P - \rho g y \\ S_{22} &= -\rho g y \\ S_{12} &= 0. \end{aligned} \tag{5}$$

The origin of the y direction is left arbitrary which is equivalent to adding an arbitrary uniform hydrostatic stress in order to suit the boundary conditions. Equations 1 to be satisfied by the incremental stress field then become

$$\begin{aligned} \frac{\partial s_{11}}{\partial x} + \frac{\partial s_{12}}{\partial y} + \rho g \frac{\partial v}{\partial x} - P\frac{\partial \omega}{\partial y} &= 0 \\ \frac{\partial s_{12}}{\partial x} + \frac{\partial s_{22}}{\partial y} - \rho g \frac{\partial u}{\partial x} - P\frac{\partial \omega}{\partial x} &= 0. \end{aligned} \tag{6}$$

The boundary conditions may be formulated using the following relations (4, 5, 6):

$$\begin{aligned} dF_x &= -[s_{12} + S_{12} - S_{22}\omega + S_{12}e_{xx} - S_{11}e_{xy}]dx \\ &\quad + [s_{11} + S_{11} - S_{12}\omega + S_{11}e_{yy} - S_{12}e_{xy}]dy \\ dF_y &= -[s_{22} + S_{22} + S_{12}\omega + S_{22}e_{xx} - S_{12}e_{xy}]dx \\ &\quad + [s_{12} + S_{12} + S_{11}\omega + S_{12}e_{yy} - S_{22}e_{xy}]dy \end{aligned} \tag{7}$$

where dF_x and dF_y are the forces acting on an element of boundary initially represented by dx, dy. The force $d\bar{F}$ is acting on matter lying on the left side of the arc dx, dy, considered as a vector differential. For the particular prestress field under consideration, Eq. 5, these relations become

$$dF_x = -\left[s_{12} + Pe_{xy} + \rho g y \frac{\partial v}{\partial x}\right] dx + \left[s_{11} - (P + \rho g y)\left(1 + \frac{\partial v}{\partial y}\right)\right] dy \quad (8)$$

$$dF_y = -\left[s_{22} - \rho g y \left(1 + \frac{\partial u}{\partial x}\right)\right] dx + \left[s_{12} - P\omega + \rho g y \frac{\partial u}{\partial y}\right] dy.$$

We must also express relations between the incremental stresses and deformations. If we assume that they are of the same form as for an unstressed medium, we write

$$s_{ij} = 2\bar{Q}e_{ij} + \delta_{ij}\bar{R}e \quad (e = e_{xx} + e_{yy}) \quad (9)$$

with the operators $\left(p = \frac{d}{dt}, \text{ time derivative}\right)$,

$$\bar{Q} = \int_0^\infty \frac{p}{p + r} Q(r)dr + Q + Q'p$$
$$\bar{R} = \int_0^\infty \frac{p}{p + r} R(r)dr + R + R'p. \quad (10)$$

We have previously derived these expressions from irreversible thermodynamics (8). Strictly speaking their use for prestressed media may involve an approximation. The nature of the limitations involved was discussed in reference 2. However, in most problems these limitations are only of academic interest.

Substitution of expression 9 for the stresses s_{ij} into Eqs. 6 yields two operational equations for the displacements u and v. The problem of deformation and folding of a layer lying on a semi-infinite medium both of heavy viscoelastic material and subject to a horizontal compression is thus reduced to solving the two simultaneous equations for u and v with appropriate boundary conditions. This can be done in a way entirely analogous to the procedure followed in reference 3. The exact solution however is somewhat involved and we have preferred to follow an approximate but much simpler approach in analogy with our treatment of the problem in reference 1.

3. APPROXIMATE SOLUTION OF THE PROBLEM

A viscoelastic layer lies on a semi-infinite medium also viscoelastic of mass density ρ_1. A force of gravity g per unit mass acts on both media and the layer is subject to a horizontal compressive stress (Fig. 1). The following assumptions are introduced:

(*a*). The layer behaves like a plate and obeys the simplified equations of the plate theory.

(*b*). The hydrostatic prestress due to gravity is the only prestress in the underlying medium.

(*c*). Interfacial adherence of the layer and medium is neglected.

(*d*). Both materials are assumed incompressible.

(*e*). The weight of the layer has no effect on the folding, i.e., the layer density may be assumed equal to zero.

The justification of assumptions (*a*) and (*b*) is established by the results in reference 3 which indicate that the factors neglected are not too significant for practical purpose. The same remark holds for assumption (*c*) on the basis of the analysis carried out in reference 2 by taking into account the adherence. Assumption (*e*) is an approximation which for physical reasons may be considered to follow from (*a*) since the plate bending occurs with no variation in thickness.

It may be expected that the assumption of incompressibility does not restrict the results significantly while providing the advantage of simplicity in the mathematical treatment.

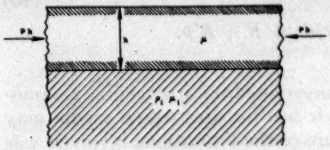

FIG. 1. Compressed layer lying on top of a heavy medium.

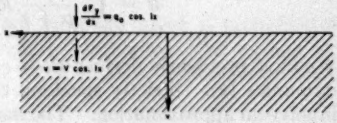

FIG. 2. Coordinates, surface forces, and deflections for the half space.

Consider first the underlying medium as an infinite half-space, the surface lying at $y = 0$, and the y axis being directed downward (Fig. 2). Since we neglect any initial horizontal compression P in the underlying medium, the equations for the displacement components u and v are obtained by putting $P = 0$ and $\rho = \rho_1$, in Eq. 6, hence,

$$\begin{aligned} \frac{\partial s_{11}}{\partial x} + \frac{\partial s_{12}}{\partial y} + \rho_1 g \frac{\partial v}{\partial x} &= 0 \\ \frac{\partial s_{12}}{\partial x} + \frac{\partial s_{22}}{\partial y} - \rho_1 g \frac{\partial u}{\partial x} &= 0. \end{aligned} \tag{11}$$

Since we are dealing with an incompressible material, we may write

$$\frac{\partial u}{\partial x} + \frac{\partial v}{\partial y} = 0. \tag{12}$$

Introducing this relation in Eq. 11, they become

$$\begin{aligned} \frac{\partial}{\partial x}(s_{11} + \rho_1 g v) + \frac{\partial s_{12}}{\partial y} &= 0 \\ \frac{\partial s_{12}}{\partial x} + \frac{\partial}{\partial y}(s_{22} + \rho_1 g v) &= 0. \end{aligned} \tag{13}$$

The boundary conditions (8) at the surface $y = 0$, when the prestress is zero ($P = 0$), become

$$\begin{aligned} \frac{dF_x}{dx} &= -s_{12} \\ \frac{dF_y}{dx} &= -s_{22}. \end{aligned} \tag{14}$$

The operators $\bar{R}$ and $\bar{Q}$ of the stress-strain relations (9) defining the viscoelastic properties of the underlying medium are designated by $\bar{R}_1$ and $\bar{Q}_1$. For an incompressible material we put (8) $\bar{R}_1 = \infty$, $e = 0$, and

$$s = \bar{R}_1 e. \tag{15}$$

Relations (9) then become

$$s_{ij} - \delta_{ij} s = 2\bar{Q}_1 e_{ij}. \tag{16}$$

If we write

$$\begin{aligned} s' &= s + \rho_1 g v \\ s_{ij}' &= s_{ij} + \delta_{ij} \rho_1 g v, \end{aligned} \tag{17}$$

Eqs. 13 are transformed into

$$\begin{aligned} \frac{\partial s_{11}'}{\partial x} + \frac{\partial s_{12}'}{\partial y} &= 0 \\ \frac{\partial s_{12}'}{\partial x} + \frac{\partial s_{22}'}{\partial y} &= 0. \end{aligned} \tag{18}$$

Relations (16) become

$$s_{ij}' - \delta_{ij} s' = 2\bar{Q}_1 e_{ij} \tag{19}$$

and the boundary condition is

$$\begin{aligned} \frac{dF_x}{dx} &= -s_{12}' \\ \frac{dF_y}{dx} - \rho_1 g v &= -s_{22}'. \end{aligned} \tag{20}$$

Equations 18 and 19 are those for a medium without initial stress. The medium thus behaves as though there were no initial stress except for a modified boundary condition 20 which contains an additional "buoyancy term"—$\rho_1 g v$.

The problem of surface deflection of a viscoelastic half-space under a sinusoidal vertical load distribution was solved in references 1 and 2. For the case of an incompressible material, a vertical load distribution

$$\frac{dF_y}{dx} = q_0 \cos lx \tag{21}$$

produces a normal deflection $v = V \cos lx$ (Fig. 2) related to the load by

$$q_0 = 2\bar{Q}_1 l V. \tag{22}$$

It was also found that in the absence of a horizontal force at the surface ($F_x = 0$) the horizontal displacement at the surface also vanishes for an incompressible material. In order to take gravity into account we have just shown that we must replace the boundary force $\frac{dF_y}{dx}$ by $\frac{dF_y}{dx} - \rho_1 g v$; hence we must replace q_0 by $q_0 - \rho_1 g V$. Relation 22 then becomes

$$q_0 = (2\bar{Q}_1 l + \rho_1 g) V. \tag{23}$$

Let us now consider the layer of thickness h. We assume that it bends as a viscoelastic plate under an axial compression P and a transverse vertical load,

$$q = -q_0 \cos lx \tag{24}$$

equal and opposite in sign to the load applied to the underlying medium. We have shown in reference 1 that the plate deflection v satisfies the equation

$$\bar{B} \frac{h^3}{12} \frac{d^4 v}{dx^4} + Ph \frac{d^2 v}{dx^2} = q \tag{25}$$

where $\bar{B}$ is the operator

$$\bar{B} = \frac{4\bar{Q}(\bar{Q} + \bar{R})}{2\bar{Q} + \bar{R}} \tag{26}$$

defining the viscoelastic properties of the layer. For an incompressible material $R = \infty$ and we have

$$\bar{B} = 4\bar{Q}. \tag{27}$$

With a sinusoidal deflection $v = V \cos lx$ after introducing expressions 22 and 24 for the load, Eq. 25 becomes

$$\tfrac{1}{3}\bar{Q}h^3l^4 - Phl^2 + 2\bar{Q}_1 l + \rho_1 g = 0. \tag{28}$$

This is the basic equation of the problem. We note that the mass density of the layer does not appear in this equation. This is due primarily to our assumption that the deformation of the layer obeys the plate bending equation and therefore does not undergo a change of thickness. Actually of course a more accurate treatment would show an influence of the layer density, but the correction due to this effect may be assumed to be small.

In the next section we shall discuss the significance of Eq. 28 in relation to the folding of the layer under the simultaneous action of the axial compression P and gravity.

4. FOLDING OF A VISCOUS LAYER LYING ON A HEAVY VISCOUS MEDIUM

We shall apply Eq. 28 for an incompressible medium to the particular case of a purely viscous layer under a horizontal compression P lying on top of another heavy viscous fluid of infinite depth. The viscosity coefficient of the layer is denoted by μ, that of the underlying medium by μ_1, and the mass density of the latter by ρ_1. The corresponding operators are

$$\begin{aligned} \bar{Q} &= \mu p \\ \bar{Q}_1 &= \mu_1 p. \end{aligned} \tag{29}$$

Relation 28 may then be written

$$\frac{\tfrac{1}{3}l^2h^2 + 2\dfrac{\mu_1}{\mu}\dfrac{1}{lh}}{1 - \dfrac{1}{l^2h^2}\dfrac{\rho_1 gh}{P}} = \frac{P}{\mu p}. \tag{30}$$

The physical interpretation of this relation lies in the significance of the variable p considered as an algebraic quantity. As pointed out in our previous work (1, 2, 3) if relation 30 is satisfied, any sinusoidal folding of wave length

$$L = 2\pi/l \tag{31}$$

has an amplitude increasing with time t, proportionally to the factor e^{pt}. We have called the dominant wave length L_d that which increases at the maximum rate. This dominant wave length corresponds to the minimum value of $P/\mu p$ on the right hand side of Eq. 30. This mini-

mum depends on two parameters, μ/μ_1 and $\rho_1 gh/P$. The latter represents the influence of gravity, as the ratio of the gravity forces to the compressive load P. The relative importance of gravity is therefore dependent on the magnitude of the horizontal compression.

We note that only the density ρ_1 of the underlying medium appears in the expression for the gravity parameter. As already pointed out this is due to our assumption that the layer behaves like a plate in flexure and therefore that there is no change in thickness. The dominant wave length L_d of the folding corresponds to values of lh for which expression 30 is a minimum. Denoting by $l_d h$ this value of lh, it is related to the dominant wave length by the relation

$$\frac{L_d}{h} = \frac{2\pi}{l_d h}. \tag{32}$$

The value of $l_d h$ is plotted as a function of $\sqrt[3]{\frac{3\mu_1}{\mu}}$ in Fig. 3 for various

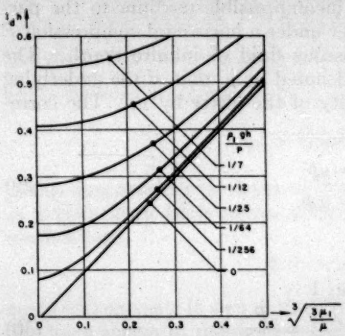

FIG. 3. The combined effect of gravity, compressive load, and viscosity on the value of $l_d h$.

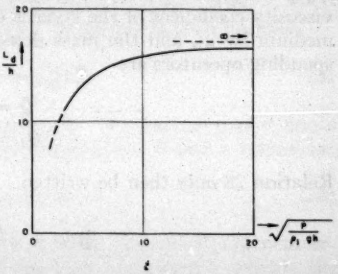

FIG. 4. The combined effect of gravity and compressive load on the dominant wave length.

values of the parameter $\rho_1 gh/P$. The case $\rho_1 gh/P = 0$ corresponds to the absence of gravity. In that case we find the straight line

$$l_d h = \sqrt[3]{\frac{3\mu_1}{\mu}}. \tag{33}$$

This is identical with the relation found in reference 1 except for the factor 3 in the present formula instead of 6. This is due to the fact that the formula of reference 1 applies to a layer embedded in a medium on both top and bottom while the present case deals with a layer lying on

the surface of a semi-infinite medium. Clearly the latter case amounts to the former if we divide by two the viscosity of the embedding medium. For $\mu_1 = 0$, that is if the underlying medium is a fluid without viscosity, the problem reduces to that of folding of a viscous plate laterally restrained only by the buoyancy of the underlying fluid. This amounts to putting $\mu_1 = 0$ in Eqs. 28 and 30. We derive

$$\frac{\mu p}{P} = \frac{3}{l^2h^2} - \frac{3\rho_1 gh}{P}\frac{1}{l^4h^4}. \tag{34}$$

The maximum of this expression as a function of lh yields the value corresponding to the dominant wave length, that is,

$$l_d h = \sqrt{\frac{2\rho_1 gh}{P}}. \tag{35}$$

These are the values plotted along the vertical axis at zero abscissa in Fig. 3. From Eq. 35 we may write for the dominant wave length due to gravity alone

$$L_d = \pi h \sqrt{\frac{2P}{\rho_1 gh}}. \tag{36}$$

For example if $P = g\rho_1 gh$, that is, if the compressive load is nine times the weight of a column of the underlying material of height equal to the layer thickness we find $L_d = 13.4 \times h$, that is, the dominant wave length due to gravity alone is about thirteen times the layer thickness.

At this point it is of interest to examine the magnitude of the instability. Following a procedure identical with that used in the previous work (2, 3) let us evaluate the factor by which the amplitude of the dominant wave length is multiplied for a period of application of the compressive load P during which the layer would undergo a compression of 25 per cent.[3] This time t_1 satisfies the relation

$$Pt_1 = 4\mu\epsilon = \mu \tag{37}$$

where the compressive strain is

$$\epsilon = \tfrac{1}{4}. \tag{38}$$

We shall examine only the case when the underlying medium has no viscosity ($\mu_1 = 0$). The amplification factor is $\exp(pt_1)$ with

$$pt_1 = \frac{3}{4}\frac{P}{\rho_1 gh}. \tag{39}$$

[3] It is of course understood that the theory is not rigorously applicable to such large deformations and the figures are only given as an indication of orders of magnitude.

In Table I we have shown the values of the amplification factor in terms of the gravity parameter.

TABLE I.

$\rho_1 gh/P$	$\exp(pt_1)$
1	2.11
1/4	20
1/7	190
1/9	850

It is seen that significant amplification occurs only for $P/\rho_1 gh \gtrsim 7$. A discussion of the amplification factor in the absence of gravity was given in references 2 and 3, and it was found that significant amplification occurred only if $\mu/\mu_1 \gtrsim 70$ that is, if $\sqrt[3]{\frac{3\mu_1}{\mu}} \gtrsim 0.35$. The range of the parameters shown in Fig. 3 corresponds to a domain for which the amplification factor is significant.

The combined effect of gravity and viscosity is completely represented by the diagram of Fig. 3. We notice that the effect of gravity dominates in regions where the wave length due to gravity alone is larger than that due to viscosity alone as determined from Eq. 33. For example, assuming a viscosity ratio $\mu/\mu_1 = 64$, we find $\sqrt[3]{\frac{3\mu}{\mu_1}} = 0.37$. The ratio L_d/h of dominant wave length to layer thickness for this case is plotted in Fig. 4 as a function of $\sqrt{\frac{P}{\rho_1 gh}}$. We see that contrary to the case where gravity is neglected the wave lengths depends on the compression P. For large values of P the ratio tends to $L_d/h = 17.2$. For the smaller values of the compressive load this ratio drops to about 12, as may be seen from the discussions in references 2 and 3. Below this value the magnitude of the instability is such that it loses its physical significance, as shown by the values of the amplification factor in Table I.

This means that in order to exhibit appreciable folding a very thick layer may require a compressive load beyond the physically possible range. This conclusion should be of significance in geological applications.

5. FOLDING OF A LAYER LYING BETWEEN TWO HEAVY MEDIA

In the previous section we have considered the layer to lie on top of another medium of infinite depth. We shall now consider the case where another medium of different density and viscosity lies on top of the layer. For simplicity the discussion is restricted to materials which are purely viscous and incompressible. We designate by ρ_1 and

μ_1 the mass density and viscosity of the bottom medium, and by ρ_2 and μ_2 the corresponding quantities for the medium lying on top. The layer of viscosity μ and thickness h under a horizontal compression P lies between those two media (Fig. 5).

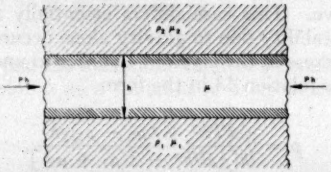

FIG. 5. Compressed layer lying between two heavy media.

We may again write Eq. 25 for the layer flexure. However in the expression of the total transverse load on the layer $q = q_0 \cos lx$ we must take into account the restraint due to top and bottom media. We therefore write in place of Eq. 23,

$$q_0 = [2(\bar{Q}_1 + \bar{Q}_2)l + (\rho_1 - \rho_2)g]V. \tag{40}$$

Since the materials are assumed purely viscous, the operators are

$$\begin{aligned} \bar{Q}_1 &= \mu_1 p \\ \bar{Q}_2 &= \mu_2 p. \end{aligned} \tag{41}$$

The sum $\bar{Q}_1 + \bar{Q}_2$ reflects the fact that the restraint of the two media on both sides of the layer is additive while $\rho_1 - \rho_2$ corresponds to the fact that the effect of gravity is subtractive. Equation 28 for the stability is therefore replaced by

$$\tfrac{1}{3}\bar{Q}h^3l^4 - Phl^2 + 2(\bar{Q}_1 + \bar{Q}_2)l + (\rho_1 - \rho_2)g = 0 \tag{42}$$

and Eq. 30 is replaced by

$$\frac{\tfrac{1}{3}l^2h^2 + 2\dfrac{\mu_1 + \mu_2}{\mu}\dfrac{1}{lh}}{1 - \dfrac{1}{l^2h^2}(\rho_1 - \rho_2)\dfrac{gh}{P}} = \frac{P}{\mu p}. \tag{43}$$

The dominant wave length is determined as before by evaluating the value of lh which minimizes this quantity. The equations are formally identical with those of the previous section except that the parameter μ_1/μ is replaced by $\dfrac{\mu_1 + \mu_2}{\mu}$ and $\rho_1 gh/P$ is replaced by $(\rho_1 - \rho_2)\dfrac{gh}{P}$.

We must distinguish two cases. In one case the bottom material is heavier than the top one, that is, $\rho_1 - \rho_2$ is positive. The dominant wave length is then determined by the same diagrams as in Figs. 3 and 4 where μ_1/μ is replaced by $(\mu_1 + \mu_2)/\mu$ and $\rho_1 gh/P$ by $(\rho_1 - \rho_2)gh/P$. In the other case the bottom material is lighter than the top one, that is, $\rho_1 - \rho_2$ is negative. This case differs essentially from the previous one in that an instability due to gravity alone occurs in the absence of any compressive stress in the layer.[4] In order to understand this more clearly let us write relation 43 in the form

$$p = \frac{Pl^2h^2 + (\rho_2 - \rho_1)gh}{lh[\frac{1}{3}\mu l^2h^2 + 2(\mu_1 + \mu_2)]}. \tag{44}$$

As pointed out above, this value of p gives a folding amplitude proportional to $\exp(pt)$ for the wave length $L = 2\pi/l$.

We see immediately that $p = \infty$, for $l = 0$, that is, the rate of folding increases indefinitely with the wave length. The reader will note that we have assumed the deformation to be very small, therefore inertia forces have been neglected. Hence, theoretically the dominant wave length is infinite. In an actual situation the surrounding medium is not infinite and the dominant wave length will be restricted by the thickness of the surrounding material. This result is of significance in geology as it is related to the formation of salt domes.

There is however the possibility of occurrence of a secondary dominant wave length due primarily to the compression P. Obviously if the effect of gravity disappears, for example if $\rho_1 = \rho_2$, there is a maximum value of p for lh equal to

$$l_d h = \sqrt[3]{\frac{3(\mu_1 + \mu_2)}{\mu}}. \tag{45}$$

This relation is found by replacing in Eq. 33 $\frac{\mu_1}{\mu}$ by $(\mu_1 + \mu_2)/\mu$. When gravity enters into the picture this maximum is displaced. This can be shown by writing Eq. 44 in the form

$$\psi = \frac{\delta^3 + \kappa}{\delta(\delta^3 + 2)} \tag{46}$$

with

$$\delta = lh\left[\frac{1}{3}\frac{\mu}{\mu_1 + \mu_2}\right]^{1/3} \tag{47}$$

[4] The stability of a stratified heavy viscous fluid has been analyzed from the viewpoint of hydrodynamics by S. Chandrasekhar (9) and R. Hide (10).

$$\kappa = \frac{(\rho_2 - \rho_1)gh}{P\left[3\left(\frac{\mu_1 + \mu_2}{\mu}\right)\right]^{2/3}} \tag{48}$$

$$\psi = \frac{P(\mu_1 + \mu_2)^{2/3}\mu^{1/3}}{\sqrt[3]{3}P}. \tag{49}$$

The problem is to find the maximum value of ψ considered as a function of δ. When we plot ψ as a function of δ we must distinguish three regions. For

$$\kappa < \tfrac{1}{2}(\tfrac{1}{4})^{2/3} = 0.198, \tag{50}$$

the plot shows a maximum and a minimum, as represented by curve 1 in Fig. 6. For

$$\kappa = \tfrac{1}{2}(\tfrac{1}{4})^{2/3}, \tag{51}$$

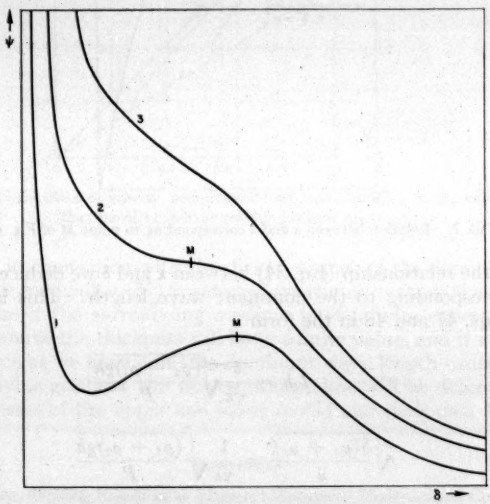

FIG. 6. Three typical curves for the dependence of ψ on δ.

the maximum and minimum coincide (curve 2) and become a horizontal inflexion point at

$$\delta = \sqrt[3]{\tfrac{1}{4}} = 0.63. \tag{52}$$

For

$$\kappa > \tfrac{1}{2}(\tfrac{1}{4})^{2/3}, \tag{25}$$

the curve has no maximum or minimum (curve 3). The point M at which the maximum of ψ occurs corresponds to a wave length of maximum rate of growth. The values of κ and δ are related at point M by the relation

$$\kappa = \frac{\delta^2(1 - \delta^2)}{2\delta^3 + 1}. \tag{54}$$

For values of κ satisfying the inequality (50) there are two positive values of δ satisfying this relation. The largest value corresponds to point M. This largest value of κ *versus* δ is plotted in Fig. 7.

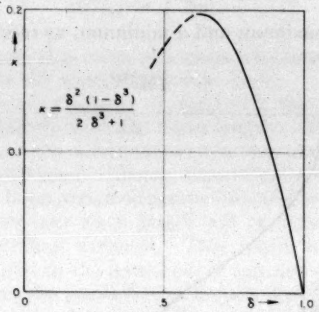

FIG. 7. Relation between κ and δ corresponding to point M of Fig. 6.

From the relationship (Eq. 54) between κ and δ we deduce the value of $l_d h$ corresponding to the dominant wave length. This is done by writing Eqs. 47 and 48 in the form

$$l_d h = \frac{\delta}{\sqrt{\kappa}} \sqrt{\frac{(\rho_2 - \rho_1)gh}{P}} \tag{55}$$

$$\sqrt[3]{\frac{3(\mu_1 + \mu_2)}{\mu}} = \frac{1}{\sqrt{\kappa}} \sqrt{\frac{(\rho_2 - \rho_1)gh}{P}}. \tag{56}$$

In these expressions κ is a function of δ through relation (54). They define a family of plots for $l_d h$ *versus* $\sqrt[3]{3(\mu_1 + \mu_2)/\mu}$ with a parameter $\sqrt{(\rho_2 - \rho_1)gh/P}$ which measures the influence of gravity. These curves are plotted in Fig. 8, in a way analogous to Fig. 3. We remember that the dominant wave length is related to $l_d h$ by Eq. 32. The interrupted line in Fig. 8 corresponds to the case where the maximum vanishes as in curve (2) of Fig. 6, hence to the disappearance of any

dominant wave length. The disappearance of the dominant wave length occurs for $\kappa > 0.198$, hence for

$$\sqrt[3]{\frac{3(\mu_1 + \mu_2)}{\mu}} > 2.25 \sqrt{\frac{(\rho_2 - \rho_1)gh}{P}}. \tag{57}$$

It will be noted that in the case of an inverse density gradient the effect of gravity is to increase the dominant wave length.

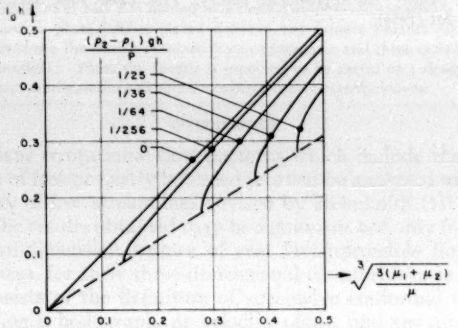

FIG. 8. Combined effect of gravity, compressive load, and viscosity, on the value of $l_0 h$ for the case of an inverse gravity gradient ($\rho_2 > \rho_1$).

Finally in connection with the disappearance of the dominant wave length if the inequality (57) is satisfied we should remark that this will only be true if the surrounding medium is of infinite extent. In actuality of course the thickness will have a finite value, and if we neglect inertia forces as we have done the dominant wave length caused by the inverse gravity gradient will not be infinite but will be determined by the thicknesses of the upper and lower media and their own boundary conditions.

REFERENCES

(1) M. A. BIOT, "Folding Instability of a Layered Viscoelastic Medium under Compression," *Proc. Roy. Soc. A.*, Vol. 242, pp. 444–454 (1957).

(2) ——, "On the Instability and Folding Deformation of a Layered Viscoelastic Medium in Compression," *J. Appl. Mech.*, in press.

(3) ——, "Folding of a Layered Viscoelastic Medium Derived from an Exact Stability Theory for the Continuum under Initial Stress," *Quart. Appl. Math.*, (in press).

(4) ——, "Nonlinear Theory of Elasticity and the Linearized Case for a Body under Initial Stress," *Phil. Mag.*, Ser. 7, Vol. XXVII, pp. 468–489 (1939).

(5) ——, "Elastizitats Theorie Zweiter Ordnung mit Anwendungen," *Zeit. Ang. Math. u. Mech.*, Vol. 20, pp. 89–99 (1940).

(6) ——, "Théorie de l'Elasticité du Second Ordre avec Application à la Théorie du Flambage," *Ann. Soc. Scient. de Bruxelles*, Vol. LIX, Ser. I, pp. 104–112 (1939).

(7) ——, "Variational and Lagrangian Methods in Viscoelasticity," in "Proc. IUTAM Colloquium on the Deformation and Flow of Solids (Madrid 1955)," Berlin, Springer, 1956.

(8) ——, "Theory of Stress-Strain Relations in Anisotropic Viscoelasticity and Relaxation Phenomena," *J. Appl. Phys.*, Vol. 25, pp. 1385–1391 (1954).

(9) S. CHANDRASEKHAR, "The Character of the Equilibrium of an Incompressible Heavy Viscous Fluid of Variable Density," *Proc. Camb. Phil. Soc.*, Vol. 51, Part 1, pp. 162–178 (1955).

(10) R. HIDE, "The Character of the Equilibrium of an Incompressible Viscous Fluid of Variable Density: An Approximate Theory," *Proc. Camb. Phil. Soc.*, Vol. 51, Part 1, pp. 179–201 (1955).

V.2
195

OBLIQUE IMPACT OF A BOUNDED STREAM ON A PLANE LAMINA

BY

TURGUT SARPKAYA [1]

ABSTRACT

In this paper, Helmholtz's free streamline theory is used to determine the contraction coefficients of two jets formed by a finite, two-dimensional stream impinging obliquely upon a plane lamina placed between two infinite parallel planes. The agreement between the results obtained from experiments and those calculated from theory is excellent. Thus, the theory is expected to be useful as a design tool for such boundary configurations as those represented by butterfly valves.

INTRODUCTION

Many plane irrotational flow patterns which include the formation or deflection of free or partly bounded jets can be analyzed satisfactorily by the theory of free streamlines devised by Helmholtz (1)[2] and Kirchhoff (2). The results obtained may be significant not only for the corresponding two-dimensional flows of real incompressible fluids, but in many instances, for their three-dimensional counterparts as well. The analysis consists of the definition of successive conformal transformations involving a hodograph, or velocity plane, and the application of Schwartz (3)–Christoffel (4) transformation. The fact should be emphasized that from the mathematical viewpoint, the direct calculation of free-streamline flows is restricted to two-dimensional irrotational flows of incompressible fluids which are free from gravitational effects and for which the solid boundaries are straight. Hence, the formation of two jets by a finite, two-dimensional stream impinging obliquely upon a fixed plane lamina placed between two infinite parallel planes (Fig. 1) is well suited to free streamline analysis because of the dominance of inertia and pressure in the establishment of the flow pattern.

The practical importance of the problem under consideration is recognized at once if the similarity of the flow pattern treated herein to that encountered in butterfly valves is noted. Butterfly valves installed in pipes or penstocks are normally used for one of two basic services: either as closure or "on-off" valves, or for flow rate control or "governing." The three major geometric variables affecting flow performance are the piping arrangement, shape of blade, and the closing angle. Available information on contraction and flow coefficients of butterfly valves is rather limited and obtained primarily from experi-

[1] Assistant Professor, Department of Engineering Mechanics, University of Nebraska, Lincoln, Nebraska.

[2] The boldface numbers in parentheses refer to the references appended to this paper.

ments conducted on two- and three-dimensional models and prototypes.

This paper includes a demonstration of the effects of geometric variables involved and presents the analytical determination of contraction and discharge coefficients for a two-dimensional butterfly valve. For the present problem since the shear is not a primary factor, for the flow accelerates rapidly, the differences between comparable ideal and real flows are small. The importance of gravitational effects for the coefficient of contraction is already known to be definitely secondary. However, the significance of the various restrictions can be shown only by comparing the calculated results with those obtained from observations of real flows.

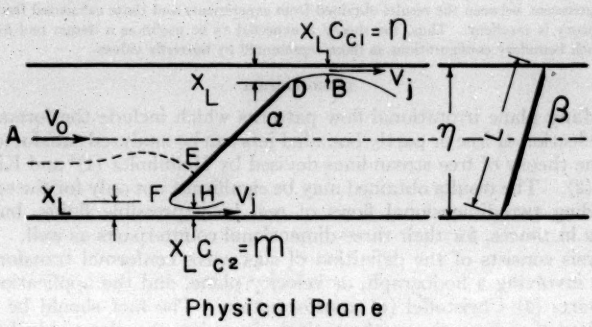

FIG. 1.

STATEMENT OF PROBLEM

Being fully aware of the restrictions and limitations of the applicability of this method, the solution of the problem under consideration proceeds as follows: If the coefficients of contraction at points B and H are C_{c1} and C_{c2}, respectively, as shown in the physical plane (Fig. 1), then the main objective of the present investigation becomes the determination of the relationships:

$$\frac{C_{c1}}{C_{c2}} = F_{1-2}(\alpha, \beta). \tag{1}$$

The existing relationships are:

$$n = C_{c1}\frac{\eta}{2}\left(1 - \frac{\sin\alpha}{\sin\beta}\right) \tag{2}$$

$$m = C_{c2}\frac{\eta}{2}\left(1 - \frac{\sin\alpha}{\sin\beta}\right) \tag{3}$$

$$\beta = \sin^{-1}\frac{\eta}{L} \tag{4a}$$

$$\frac{n}{m} = \frac{C_{c1}}{C_{c2}} \tag{4b}$$

$$\frac{V_0}{V_j}\frac{2}{1-\dfrac{\sin\alpha}{\sin\beta}} = C_{c1} + C_{c2} \tag{5}$$

in which n and m represent the thickness of the jets at B and H, respectively; η is the width of channel; β is the angle of closure; α is the variable angle; and L is the length of valve plate. The velocities of both jets are equal to V_j and the velocity far upstream from the valve plate is V_0.

If z and w are used for the complex variable and the complex potential, then the variable ζ defined as (dw/dz) is given by

$$\zeta = -u + iv = -qe^{-i\theta} \tag{6}$$

in which u and v are the velocity components in the x and y directions, q is the magnitude of the velocity vector, and θ is the angle of its inclination.

If the variable Ω,

$$\Omega = Ln\left(-\frac{V_j}{\zeta}\right) = -Ln\frac{q}{V_j} + i\theta \tag{7}$$

is introduced, the flow region in the physical plane (Fig. 1) can be mapped onto a corresponding region in the Ω-plane, as indicated in Fig. 2. Either ζ or Ω must be related to w by means of known methods

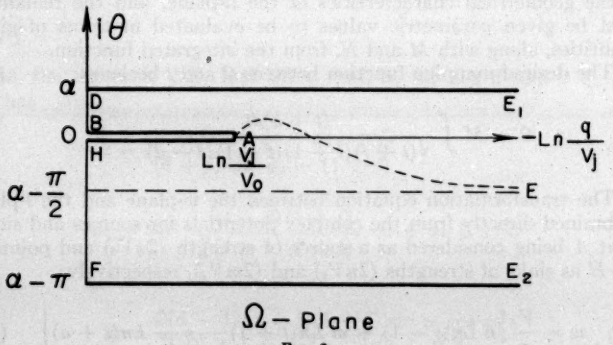

FIG. 2.

through still another complex variable designated as t. This relationship completes the rather complicated functional analysis because, as has already been seen, either ζ or Ω can be expressed in terms of (dw/dz).

Any polygonal boundary in one complex plane can be transformed into the entire real axis of another through application of Schwartz-Christoffel theorem, the interior of the polygon being transformed into either the upper or the lower half of the second plane. Thus, the outline in the Ω-plane is directly transformable into the real axis of the t-plane. Therefore, if we open out the Ω-plane and lay it along the real axis of the t-plane as shown in Fig. 3, the interior of the Ω-plane trans-

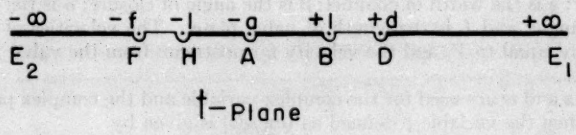

FIG. 3.

forms into the lower half of the t-plane. The transforming function can be written as follows:

$$\Omega = M \int \frac{dt}{(t - t_1)^{\gamma_1/\pi}(t - t_2)^{\gamma_2/\pi} \dots} + N. \tag{8}$$

As many factors $(t - t_n)$ are introduced into the transformation as there are vertices of the polygonal boundary in the Ω-plane. The value t_n is the locus of the transformed point on the real axis in the t-plane, and γ_n is the exterior angle of the polygon at that point in the t-plane. Three of the t_n values can be assigned arbitrarily but with due regard to the geometrical characteristics of the Ω-plane, and the remainder must be given parametric values to be evaluated in terms of given quantities, along with M and N, from the integrated function.

The desired mapping function between Ω and t becomes:

$$\Omega = M \int \frac{(t + a)dt}{\sqrt{(t + f)(t + 1)(t - 1)(t - d)}} + N. \tag{9}$$

The transformation equation between the w-plane and the t-plane is obtained directly from the complex potentials for sources and sinks, point A being considered as a source of strength $(2\eta V_0)$ and points B and H as sinks of strengths $(2nV_j)$ and $(2mV_j)$, respectively:

$$w = \frac{V_j}{\pi}\left\{n\,Ln(t - 1) + m\,Ln(t + 1) - \eta\frac{V_0}{V_j}Ln(t + a)\right\} \tag{10}$$

or

$$w = \frac{\eta V_j}{2\pi}\left(1 - \frac{\sin\alpha}{\sin\beta}\right)$$

$$\times\{C_{e1}\,Ln(t-1) + C_{e2}\,Ln(t+1) - (C_{e1}+C_{e2})\,Ln(t+\mathrm{a})\} \quad (10a)$$

and w is connected to z by the relation

$$z = -\frac{1}{V_j}\int e^{0} dw. \quad (11)$$

The integral given by Eq. 9 can be decomposed into two component integrals:

$$\Omega = M\int \frac{t\,dt}{\sqrt{(t^2-1)(t-d)(t+f)}} + M\int \frac{a\,dt}{\sqrt{(t^2-1)(t-d)(t+f)}} + N. \quad (12)$$

EXAMPLES

Let us consider the transformation of Legendre (5):

$$t = \frac{a_0 \sin^2\phi + b_0}{c_0 \sin^2\phi + d_0}. \quad (13)$$

a_0, b_0, c_0, and d_0 can be so chosen that the above integrals simplify and reduce to known integrals. It should be noted that these integrals, depending on the values of t require separate treatment for each interval under consideration.

Case I

In the intervals DE_1 and FE_2, that is, for $t \geqslant d$ and $t \leqslant -f$, one has

$$t = \frac{(d+f)\sin^2\phi_1 - d(1+f)}{(d+f)\sin^2\phi_1 - (1+f)} \quad (14)$$

$$\phi_1 = \sin^{-1}\sqrt{\frac{(t-d)(1+f)}{(t-1)(d+f)}}, \quad 0 \leqslant \phi_1 \leqslant \pi/2, \quad (15)$$

and

$$dt = \frac{2(d-1)(d+f)(1+f)\sin\phi_1\cos\phi_1}{[(d+f)\sin^2\phi_1 - (1+f)]^2}. \quad (16)$$

If Eqs. 14 and 16 are replaced in Eq. 12, one obtains

$$\Omega = \int \frac{2M}{\sqrt{(1+f)(1+d)}} \frac{(d+f)\sin^2\phi_1 - d(1+f)}{(d+f)\sin^2\phi_1 - (1+f)} \frac{d\phi_1}{\sqrt{1-k_1^2\sin^2\phi_1}} + \int \frac{2Ma}{\sqrt{(1+f)(1+d)}} \frac{d\phi_1}{\sqrt{1-k_1^2\sin^2\phi_1}} + N. \quad (17)$$

Integral 17 can be separated into a first and third kind elliptic integral:

$$\Omega = \frac{2M}{\sqrt{(1+f)(1+d)}} \left\{ (1+a)F(\phi_1, k_1) + (d-1)\Pi_L\left(\phi_1, -\frac{d+f}{1+f}, k_1\right) \right\} + N. \quad (18)$$

$\Pi_L(\phi_1, n, k)$ is the third kind elliptic integral of Legendre, and may be written as

$$\Pi_L(\phi_1, n, k) = \int \frac{d\phi_1}{(1+n\sin^2\phi_1)\sqrt{1-k^2\sin^2\phi_1}}. \quad (19)$$

The parameter n is taken as real, and may take any value, positive or negative. For the intervals under consideration,

$$n_1 = -\frac{d+f}{1+f} \qquad -\infty < n_1 < -1.$$

Legendre's integral is connected with Jacobi's by the relation

$$\Pi_L(\phi_1, n_1, k_1) = u_1 - \frac{sn(\epsilon_1, k_1)}{cn(\epsilon_1, k_1)dn(\epsilon_1, k_1)} \Pi_j(u_1, \epsilon_1 + iK') \quad (20)$$

in which u_1 is written for $F(\phi_1, k_1)$. sn, cn and dn are elliptic functions and K' is the complete elliptic integral of the first kind for the complementary modulus. ϵ_1 is given by the relation

$$n_1 = -\frac{d+f}{1+f} = -k_1^2 sn^2(\epsilon_1 + iK', k_1) = -\frac{1}{sn^2(\epsilon_1, k_1)}$$

and

$$sn^2\epsilon_1 = \frac{1+f}{d+f}, \quad cn^2\epsilon_1 = \frac{d-1}{d+f}, \quad dn^2\epsilon_1 = \frac{d-1}{d+1}.$$

In order to simplify the notations, $sn(\epsilon_1, k_1)$, $cn(\epsilon_1, k_1)$ and $dn(\epsilon_1, k_1)$ will be denoted by $sn\epsilon_1$, $cn\epsilon_1$, and $dn\epsilon_1$, respectively.

The solution of Jacobi's integral is given by

$$\Pi_j(u_1, \epsilon_1 + iK') = u_1 Z(\epsilon_1, k_1) + \frac{u_1 cn\epsilon_1 dn\epsilon_1}{sn\epsilon_1} + \tfrac{1}{2} Ln \frac{H(\epsilon_1 - u_1)}{H(\epsilon_1 + u_1)} \quad (21)$$

in which $H(\epsilon_1 \pm u_1)$ is Jacobi's Theta-function (6), and

$$k_1^2 = \frac{2(f+d)}{(1+f)(1+d)}.$$

Hence Legendre's integral becomes:

$$\Pi_L(\phi_1, n_1, k_1) = -\frac{sn\epsilon_1}{cn\epsilon_1 \cdot dn\epsilon_1}\left\{u_1 Z(\epsilon_1, k_1) + \tfrac{1}{2} Ln \frac{H(\epsilon_1 - u_1)}{H(\epsilon_1 + u_1)}\right\}. \quad (22)$$

From Eqs. 18 and 22, we have

$$\Omega = \frac{2M}{\sqrt{(1+f)(1+d)}}\left\{(1+a)u_1 - (d-1)\frac{sn\epsilon_1}{cn\epsilon_1 \cdot dn\epsilon_1} \times \left[u_1 Z(\epsilon_1, k_1) + \tfrac{1}{2} Ln \frac{H(\epsilon_1 - u_1)}{H(\epsilon_1 + u_1)}\right]\right\} + N \quad (23)$$

which is the solution sought for the intervals under consideration. The constants M and N are determined from the comparison of Ω- and t-planes for the corresponding values and were found to be 1 and $i\alpha$, respectively.

Case II

For the interval HB, that is, $|t| < 1$, if t is taken as

$$t = \frac{-2f \sin^2 \phi_2 + (1+f)}{2 \sin^2 \phi_2 - (1+f)} \quad (24)$$

and the foregoing manipulations repeated, one obtains

$$\Omega = \frac{2M}{\sqrt{(1+d)(1+f)}}\left\{(a-f)F(\phi_2, k_2) + (f-1)\Pi_L\left(\phi_2, -\frac{2}{1+f}, k_2\right)\right\} \quad (25)$$

in which $n_2 = -\dfrac{2}{1+f}$ which varies between zero and $-k_2^2$. Writing $u_2 = F(\phi_2, k_2)$ and $n_2 = -k_2^2 sn^2(\epsilon_2, k_2) = -\dfrac{2}{1+f}$, one has

$$\Pi_L = u_2 + \frac{sn\epsilon_2}{cn\epsilon_2 \cdot dn\epsilon_2}\left\{u_2 Z(\epsilon_2, k_2) + \tfrac{1}{2} Ln \frac{\theta(\epsilon_2 - u_2)}{\theta(\epsilon_2 + u_2)}\right\} \quad (26)$$

and therefore

$$\Omega = \frac{2}{\sqrt{(1+d)(1+f)}}\left\{(a-1)U_2 + (f-1)\frac{sn\epsilon_2}{cn\epsilon_2 \cdot dn\epsilon_2} \times \left[u_2 Z(\epsilon_3) + \tfrac{1}{2}Ln\frac{\theta(\epsilon_2 - u_2)}{\theta(\epsilon_2 - u_2)}\right]\right\} \quad (27)$$

in which

$$k_2 = k_1 = \sqrt{\frac{2(f+d)}{(1+f)(1+d)}} \qquad \phi_2 = \sin^{-1}\sqrt{\frac{(1+f)(1+t)}{2(t+f)}}$$

$$k_2' = k_1' = \sqrt{\frac{(d-1)(f-1)}{(d+1)(f+1)}}$$

and

$$sn\epsilon_2 = \sqrt{\frac{1+d}{f+d}}, \quad cn\epsilon_2 = \sqrt{\frac{f-1}{f+d}}, \quad dn\epsilon_2 = \sqrt{\frac{f-1}{f+1}}.$$

$\theta(\epsilon \pm u)$ also is Jacobi's Theta-function and connected to $H(\epsilon \pm u)$ by the relation $\theta(z + iK') = iBH(z)$ where

$$Ln\, B = \frac{\pi K'}{4K} - \frac{\pi i z}{2K}.$$

K and K' are complete elliptic integrals of the first kind connected by the following relationships:

$$K = sn^{-1}(1, k), \quad K' = sn^{-1}(1, k') = sn^{-1}(1, \sqrt{1-k^2}).$$

Case III

For the interval BD, that is, $1 < t \leqslant d$, if t is taken as

$$t = -\frac{(d-1)\sin^2\phi_3 + (1+d)}{(d-1)\sin^2\phi_3 - (1+d)} \quad (28)$$

one obtains

$$\Omega = \frac{2M}{\sqrt{(1+f)(1+d)}}\left\{(a-1)u_3 + 2\Pi_L\left(\phi_3, -\frac{d-1}{d+1}, k_3\right)\right\} + N. \quad (29)$$

Repeating the intermediate manipulations, one has

$$\Omega = \frac{2M}{\sqrt{(1+f)(1+d)}} \left\{ (a+1)u_3 + 2\frac{sn\epsilon_3}{cn\epsilon_3 \cdot dn\epsilon_3} \times \left[u_3 Z(\epsilon_3) + \tfrac{1}{2} Ln \frac{\theta(\epsilon_3 - u_3)}{\theta(\epsilon_3 + u_3)} \right] \right\} + N \quad (30)$$

in which

$$k_3^2 = \frac{(d-1)(f-1)}{(d+1)(f+1)} = k_2'^2, \quad k_3'^2 = k_1^2 = k_2^2 = \frac{2(d+f)}{(1+f)(1+d)}$$

and

$$n_3 = -k_3^2 sn^2(\epsilon_3, k_3) = -\frac{d-1}{d+1}, \quad -k_3^2 \leqslant n_3 \leqslant 0$$

$$sn\epsilon_3 = \sqrt{\frac{f+1}{f-1}}, \quad cn_3 = i\sqrt{\frac{2}{f-1}}, \quad dn_3 = \sqrt{\frac{2}{d+1}}$$

and

$$\phi_3 = \sin^{-1}\sqrt{\frac{(d+1)(t-1)}{(d-1)(t+1)}}.$$

Case IV

For the interval FH, that is, $-1 \geqslant t \geqslant -f$, if t is taken as

$$t = \frac{d(f-1)\sin^2\phi_4 - f(d+1)}{(f-1)\sin^2\phi_4 + (d+1)} \quad (31)$$

one obtains

$$\Omega = \frac{2M}{\sqrt{(1+f)(1+d)}} \left\{ (d+a)u_4 - (d+f)\Pi_L\left(\phi_4, \frac{f-1}{d+1}, k_4\right) \right\} \quad (32)$$

in which

$$n_4 = \frac{f-1}{d+1} > 0, \quad n_4' = -k_4 sn^2(i\epsilon_4, k_4) = k_4^2 sn^2(\epsilon_4, k_4')/cn^2(\epsilon_4, k_4')$$

$$n_4 = k_4^2 \tan^2\theta, \quad \sin\theta = sn(\epsilon_4, k_4').$$

Thus,

$$\Omega = u_4 + \frac{sn(\epsilon_4, k_4) \cdot cn(\epsilon_4, k_4)}{dn(\epsilon_4, k_4)} \left\{ iu_4 Z(i\epsilon_4) - i\tfrac{1}{2} Ln \frac{\theta(u_4 - i\epsilon_4)}{\theta(u_4 + i\epsilon_4)} \right\}. \quad (33)$$

From Eqs. 32 and 33, one has

$$\Omega = \frac{2M}{\sqrt{(1+d)(1+f)}} \left\{ (a-f)u_4 - (d+f)\frac{sn(\epsilon_4, k_4')\cdot cn(\epsilon_4, k_4')}{dn(\epsilon_4, k_4')} \times \left[iu_4 Z(i\epsilon_4) + i\tfrac{1}{2} Ln \frac{\theta(u_4 - i\epsilon_4)}{\theta(u_4 + i\epsilon_4)} \right] \right\} + N \quad (34)$$

in which

$$u_4 = F(\phi_4, k_4), \quad k_3'^2 = k_4'^2 = \frac{2(d+f)}{(1+f)(1+d)}$$

$$k_4^2 = \frac{(d-1)(f-1)}{(d+1)(f+1)}, \quad sn(\epsilon_4, k_4') = \sqrt{\frac{f+1}{f+d}}, \quad cn(\epsilon_4, k_4') = \sqrt{\frac{d-1}{f+d}}$$

and

$$dn(\epsilon_4, k_4') = \sqrt{\frac{d-1}{d+1}}, \quad \epsilon_4 = sn^{-1}\left\{ \sin\left(\tan^{-1}\sqrt{\frac{f+1}{d-1}} \right) \right\}.$$

Intermediate steps in the solutions of the above integrals have been omitted for the sake of brevity. In order to obtain z from Eq. 11, dw

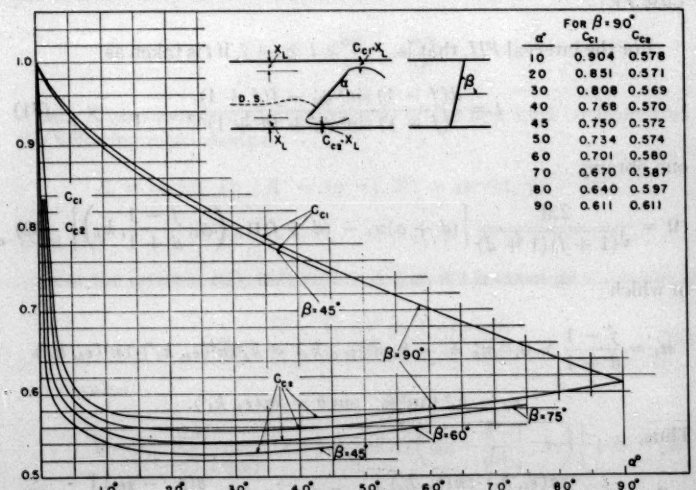

FIG. 4.

should be written as

$$dw = \frac{\eta V_j}{2\pi}\left(1 - \frac{\sin\alpha}{\sin\beta}\right)\left(\frac{C_{c1}}{t-1} + \frac{C_{c2}}{t+1} - \frac{C_{c1}+C_{c2}}{t+a}\right)dt. \quad (35)$$

The rest of the integration could only be performed by numerical methods. The best and well-known method for this purpose is King's (7) A. G. M. scale method. If for a fixed value of β, numerical values are assigned to a, f and d, satisfying the boundary conditions in the transformed planes, corresponding simultaneous values may be obtained for C_{c1}, C_{c2} and α.

The results or the functional relationships obtained from these equations are shown in Fig. 4. The significance of this figure is obvious. The contraction coefficient C_{c1} varies greatly with α, but very little with the angle of complete closure β, whereas the contraction coefficient C_{c2} varies appreciably with β, but very little with α, for the values of α greater than approximately 15°. But for small values of the variable angle α, C_{c2} varies extremely fast and approaches unity. The values of the corresponding angles (corresponding to $\alpha < 10°$) used in evaluating the elliptic functions approach their limit so closely that difficulties are encountered because of limitations in the tables available.

THEORY *VERSUS* EXPERIMENTS

In order to compare the theoretical results with those obtained from experiments it is necessary to compute the discharge coefficient from theoretically determined contraction coefficients since it is the most accustomed and widely used coefficient and more readily determined experimentally. The rate of flow and the total head are expressed by

$$Q = V_0 A = C_Q A\sqrt{g\Delta H} \quad (36a)$$

$$\Delta H = \frac{V_j^2}{2g} \quad (36b)$$

in which A is the area of the normal cross-section of the approach channel, and C_Q the coefficient of discharge. Combining Eqs. 36*a* and 36*b* with Eq. 5, the coefficient of discharge is obtained easily as

$$C_Q = \frac{\pi}{4\sqrt{2}}(C_{c1} + C_{c2})\left[1 - \frac{\sin\alpha}{\sin\beta}\right]. \quad (37)$$

C_Q values computed from Eq. 37 for $\beta = 75°$ using the contraction coefficients obtained in Fig. 4, are plotted in Fig. 5, and the solid line is obtained. In the same figure the experimental data taken from reference (8) are also plotted. The agreement between the theoretical and

experimental results is fairly good, the theoretical discharge coefficient being somewhat smaller.

A similar computation has been made for $\beta = 90°$, and the resultant theoretical curve with the experimental points taken from reference (9) are shown in Fig. 6. The agreement between the theoretical and experimental results is excellent.

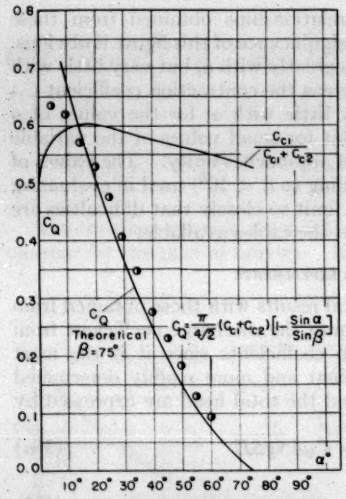

FIG. 5.

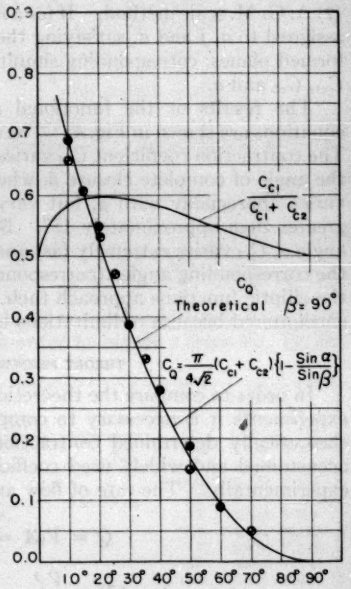

FIG. 6.

STABILITY OF FLOW

So far we have dealt with the effects of geometric variables on each coefficient of contraction and on discharge coefficient. It is seen that the coefficients of contraction are functions of α and β only, and do not depend on the magnitude of the rate of flow.

The second point we propose to discuss is the stability of flow for various positions of lamina and in connection with this the explanation for the scatter of experimental data for very small values of α or for near-full open positions of lamina. The stability of flow depends on the stability of the stagnation point or rather specifically speaking of the stagnation line on the valve plate. As α becomes smaller, the stag-

nation line approaches the lower edge of the valve plate and theoretically it reaches the edge when α is zero. But, practically the stagnation point or line reaches the sharp end of the plate when α becomes about 15°. To illustrate this, a curve has been drawn computing the location of the stagnation point for $\beta = 90°$ and for various values of α, as shown in Fig. 7. The dimensionless parameter λ becomes practically zero for $\alpha = 20°$.

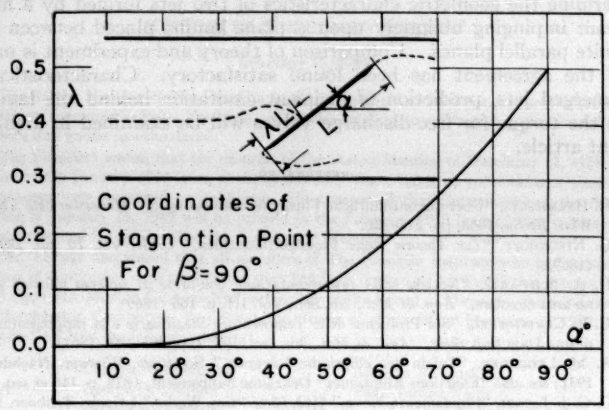

FIG. 7.

In the case of axially symmetrical flow, the locus of stagnation points is curvilinear. Therefore, the stagnation points in the vicinity of valve axis are very close to the edge of valve plate, whereas the stagnation points in the vicinity of the diameter perpendicular to the valve axis are relatively far from the edge. Therefore, it is very likely that in the case of axially symmetrical flow for a critical value of α the stagnation points relatively near the plate edge jump abruptly to the edge of the plate changing the discharge coefficient. In the two-dimensional case the entire stagnation line jumps abruptly to the edge of the plate for small values of α. For a critical value of α, however, the stagnation line is unstable and jumps to the edge and then back alternately resulting in unstable flow.

It seems to be evident from the foregoing explanation that the scatter of the experimental data for small values of α is largely due to the rapid and abrupt variations in the location of stagnation point in that region. Moreover, the geometry of valve plate also has an important effect on the variations of aforementioned coefficients. Theoretically, the plate is a thicknessless lamina, but practically it has a

finite thickness. Therefore, for a blade with a relatively wide tip, the point of separation will be at one or the other edge, depending upon the relative blade angle. The sudden slight shift of discharge coefficient for some valves is due to this transfer of the separation point.

SUMMARY

In this paper, Helmholtz's free streamline theory has been used to determine the geometric characteristics of two jets formed by a finite stream impinging obliquely upon a plane lamina placed between two infinite parallel planes. Comparison of theory and experiment is made and the agreement has been found satisfactory. Characteristics of submerged jets, prediction of incipient cavitation behind the lamina, and the torque for free-discharge valves will be examined in a subsequent article.

REFERENCES

(1) H. HELMHOLTZ, "Uber discontinuirliche Flussigkeitsbewegungen," *Monatsberichte Akad d. Wiss. Berlin*, 1868, pp. 215–228.
(2) G. KIRCHHOFF, "Zur Theorie freier Flussigkeitsstrahlen," *Crelle*, Vol. 70, pp. 289–298 (1869).
(3) H. A. SCHWARTZ, "Notizia sulla rappresentazione conforme di un'area ellittica sopra un'area circolare," *Ann. di Mat.*, 2da Ser., Vol. III, p. 166 (1869).
(4) E. B. CHRISTOFFEL, "Sul Problema delle Temperature Stazionarie e la rappresentazione di una Data Superficie," *Ann. di Mat.*, 2da Ser., Vol. I, pp. 95–103 (1867).
(5) A. M. LEGENDRE, "Tafeln der elliptische Integrale," Stuttgart, Wittwer, Nachdruck, 1931; see also "Fonctions Elliptiques" Deuxieme Supplement, 1828, p. 146 et seq.
(6) C. G. J. JACOBI, "Fundamenta Nova," §§62, 63 of "Ges. Werke," Leipzig, Teubner, 1881, Bd.11, pp. 229–231; see also A. CAYLEY, "Elliptic Functions," Second Edition, London, Leyton, 1895, Chap. VI.
(7) L. V. KING, "On the Direct Numerical Calculation of Elliptic Functions and Integrals," Cambridge University Press, 1924.
(8) M. B. MCPHERSON, H. S. STRAUSSER AND J. C. WILLIAMS, "Butterfly Valve Flow Characteristics," *Proc.*, Am. Soc. Civil Engrs., Vol. 83 (J. Hydraulics Div.), HYI, Feb. 1957, paper No. 1167, 28 pages.
(9) D. GADEN, "Contribution à l'étude des vannes-papillons," *Schweizerische Bauzeitung*, Vol. XXVI, pp. 262–268, 275–277, 291–295 (1938).

THE FRANKLIN INSTITUTE

MINUTES OF THE STATED MEETING

February 18, 1959

The Stated Meeting of The Franklin Institute was held at 8:15 P.M. in the Lecture Hall. Mr. Wynn Laurence LePage, President, called the meeting to order with approximately 300 members and guests in attendance.

The President stated that the minutes of the Stated Meeting of December 17, 1958 were printed in the January 1959 issue of the JOURNAL. There being no corrections or additions, the minutes were approved as published. He announced that the minutes of the Annual Meeting of January 21, 1959 will be printed in the February 1959 issue of the JOURNAL and will be presented for approval at the next Stated Meeting.

Mr. LePage announced that all members of The Franklin Institute who had completed 25 years of continuous membership last year had been invited as our guests this evening. He called upon Mr. Morton Gibbons-Neff, a member of the Board of Managers and Chairman of the Membership Committee, to present the names of these Silver Members of 1958. Mr. Gibbons-Neff read the following names:

Charles A. Bareuther	Annetta R. Masland
George E. Crofoot	Ellen-Jarden Nolde
George S. Gardner	J. Livingston Poultney
Walter H. Hartung	George A. Smith
Karl S. Howard	Floyd T. Tyson
Edward R. Hughes	Wilfred H. Wickersham

Mr. LePage then announced that this evening would mark the Fourth Annual Philip C. Staples Lecture. This lecture was established by friends of Mr. Staples, late president of The Franklin Institute and the Bell Telephone Company, as a most fitting memorial to a man who had done so much not only for The Franklin Institute but for the community in which he lived.

He introduced the speaker of the evening, Mr. H. Thomas Hallowell, Jr., President of Standard Pressed Steel Company of Jenkintown, Pennsylvania, whose subject, "Now It's Got To Work" explained why high reliability design and execution is so necessary. Mr. Hallowell's talk placed emphasis on the reliability factor, so necessary today because of the manifold parts and units that go into making up the equipment used in the home, in industry, in transportation, in our military operations and in other facets of our every-day life. An interesting film produced by Standard Pressed Steel Company illustrated his talk. Mr. Hallowell spoke of the desirability of The Franklin Institute, as a neutral organization, taking the lead in arranging for a Symposium on this subject, to include Government agencies, industries and technical societies.

Interest in Mr. Hallowell's subject was very evident by the half-hour question period and the applause following his talk. After thanking Mr. Hallowell for his very interesting talk, the President adjourned the meeting at 9:55 P.M.

WILLIAM F. JACKSON, JR.
Secretary

MEMBERSHIP

1958 SILVER MEMBERS HONORED

At the Stated Meeting on February 18, 1959, the Institute honored twelve of its members who had completed 25 consecutive years of membership. Prior to the meeting, the four new Silver Members who were able to attend were guests of honor at a dinner and reception. During dinner, Wynn Laurence LePage, President of the Institute, introduced these honored guests: George S. Gardner, Karl S. Howard, Miss Annetta R. Masland and Floyd T. Tyson. As souvenirs of the occasion, the new Silver Members received initialled paper weights containing 1958 quarters, presented to them by Morton Gibbons-Neff, Chairman of the Membership Committee. Mr. Neff read the names of the twelve new Silver Members at the Stated Meeting following the dinner.

BRIEF BIOGRAPHICAL NOTES ON THE 1958 SILVER MEMBERS

CHARLES A. BAREUTHER—Chairman of the Physics Department of the Central High School of Philadelphia and Professor Emeritus of the Evening College of Drexel Institute of Technology.

GEORGE S. CROFOOT—Retired Professor of Mechanical Engineering at the University of Pennsylvania.

GEORGE S. GARDNER—Research Chemist at Amchem Products Inc., who has contributed articles on corrosion and inhibition to this JOURNAL.

WALTER H. HARTUNG—Professor and Chairman of Chemistry and Pharmaceutical Chemistry at the Medical College of Virginia.

KARL S. HOWARD—Retired Vice President of General Steel Castings Corporation; now Consultant to the U. S. Army Ordnance Tank-Automotive Command in Detroit.

EDWARD R. HUGHES—Electrical Engineer who specializes in patent work ranging from refrigerators to weeping dolls.

ANNETTA R. MASLAND—Retired biology teacher who taught in West Philadelphia High School and Overbrook High School.

ELLEN-JARDEN NOLDE—Psychologist connected with testing programs in various Philadelphia schools; United Nations correspondent for weekly newspapers.

J. LIVINGSTONE POULTNEY—Retired Consulting Engineer for the Brill Corporation.

GEORGE A. SMITH—Patent lawyer and Partner in the firm of Busser, Smith and Harding.

FLOYD T. TYSON—Professor of Chemistry at Temple University.

WILFRED H. WICKERSHAM—Resident of Nutley, N. J.

V.2
195

NEW MEMBERS

The following elections were approved on February 5, 1959 by the Membership Committee by authority given to it by the Board of Managers.

ANNUAL

Jacques D. Bambling
Francis J. Bonner
Carl Richard Borson
Newman Bortnick
Ralph D. Bradway
Daniel B. Campbell
James B. Chambers
F. W. Chapman, Jr.
Charles W. Charny
Ellis E. Comfort
John A. Cost
Jack Dickstein
Hans O. Dietze
Joseph N. DuBarry, IV
Kenneth V. Duncan
William Ehrich
John L. Frost
Loren E. Gaither
H. Paul Gant
Augustine M. Garcia
Miro A. Grottger
John E. Jednacz
Charles H. Justice
Nelson J. Katz
Lucien Katzenberg, Jr.
Jerome W. Kaufman
James H. Keegan
Clyde M. Keitt
Louis W. Kellman
Calvin F. Kendig
Walter S. Kenworthy
Charles R. King
Lester Kiriloff
L. R. Kirkwood
T. S. Klingeman
Howard S. Kneedler, Jr.
Karl F. Koehler
Louis Kolodin
Charles E. Kunz
James A. Mallon
John Massier
J. Grant McCabe, III
Richard S. Lee
Richard S. Loveland
Thomas J. McCann
Carl V. McCarty
Harry Luecke
William Metcalf
Howard R. Milligan
Charles P. Neidig
Arnold N. Parris
Charles L. Register
George F. Rickert
Henry L. Rothman
Paxton G. Seabury
John L. Tetley
Richard T. Urffer
Maria Giulia Vitelli
Irwin Frank Wertleib
Joseph T. Wolpert, Sr.
Ernest R. Wortmann

EDUCATOR

John F. Harvey
Fred M. Hofkin
Howard B. Tansley
Hsiu Huo Yuen

NON-RESIDENT

Julian M. Avery
B. Ward Deutschman
Benjamin A. Oxnard

NECROLOGY

Seth Bunker Capp '11
Elizabeth B. Chew '36
J. S. Curley '36
Edwin H. Dressel '45
E. Monroe Fisher '52
Margaret Horstmann Packard '35
Mrs. Benjamin Rush, Sr. '36
Charles S. Redding '26
Charles H. Schaefer '43

The following are Silver Members, having belonged continuously for twenty-five years or more. The dates are years of election to membership.

1910
Richard P. Brown
Joseph S. Hepburn
Joseph W. Lippincott
J. D. Shattuck
J. M. Weiss

1912
James Barnes
Morris Llewellyn Cooke
Edwin Elliot
Walter Palmer
Julian S. Simsohn
Howard S. Worrell

1913
Sterling H. Bunnell
Irenee duPont
S. B. Eckert
Ralph E. Flanders
N. E. Funk
Lionel F. Levy
E. Mallinckrodt, Jr.
Frank M. Masters
Franklin P. McConnell
William Maul Measey
W. Chattin Wetherill
D. Robert Yarnall

1914
Russell L. Brinton
George S. Crampton
Ernest L. Huff
K. G. Mackenzie
George Wharton Pepper

1915
Thomas D. Cope
John C. Cornelius, Jr.
H. Jermain Creighton
Thomas W. Elkinton
Richard Howson
W. Wallace McKaig

1916
Henry B. Allen
James G. Detwiler
Zay Jeffries
Frank H. Sauer
B. E. Shackelford
Arthur Synnestvedt
Charles N. Weyl

1917
A. D. Chambers
Francis J. Chesterman
Walter S. Crowell
William J. Fitzmaurice, Jr.
Rolfe E. Glover, Jr.
Harold Goodwin, Jr.
Arthur W. Lowe
Frank S. MacGregor
Francis F. Milne, Jr.
C. H. Quinn
Sylvan D. Rolle
Robert L. Wood
Henry Woodhouse

1918
Charles H. Colvin
Walter O. Snelling

1919
Charles E. Brinley
Henry Colvin, 2nd
E. A. Eckhardt
George W. Furness
Frank H. Griffin
Hiram S. Lukens
J. Howard Pew
Edmund G. Robinson
L. K. Sillcox

1920
Robert Cameron Colwell
Chester Lichtenberg
P. S. Lyon
Haviland H. Platt
Carl D. Pratt

1921
Roland L. Andreau
Leonard T. Beale
J. Ed. Brewer
Arthur L. Day
Frederic Palmer, Jr.
Howard Stoertz
James Stokley
Edward R. Weidlein
S. Weinberg

1922
C. Douglas Galloway
Joseph F. Greene
C. E. K. Mees

1923
Henry Clay Gibson
Howard S. Levy
William C. Melcher, Jr.
John F. Metten
Richard G. Sagebeer
H. Birchard Taylor
Francis B. Vogdes
Joseph J. Vogdes

1924
Peter Abrams
William G. Ellis
T. R. Harrison
Valentine Hiergesell
Karl F. Oerlein
Edward B. Patterson
Nicholas G. Roosevelt
Alfred O. Tate
James Lloyd Weatherwax
Alexander Wilson, 3rd
William Zimmermann

1925
Jack G. Binswanger
Marion Eppley
John Graham Foley
J. V. Giesler
C. R. Kraus
H. F. Porter
W. F. G. Swann

1926
Charles B. Bazzoni
Neils Bohr
O. E. Buckley
William Findlay Downs
Henry C. Evans
Edward L. Forstall
Lewis H. Hendrixson
Charles S. Leopold
Alfred L. Loomis
J. H. Manning
Clement B. Newbold
O. M. Patton
Dexter N. Shaw

V.2
195

1926 (cont.)
Sydney L. Wright
Charles S. Wurtz, Jr.

1927
T. K. Cleveland
William DeKrafft
Hiram B. Ely
Leslie Griscom
Alfred Iddles
John Van Gasken Postles
Philip Sporn
Charles A. Stanwick
Charles A. Young

1928
William R. Dohan
Walton Forstall, Jr.
C. W. Hansell
Walter A. MacNair
Fred P. Nabenhauer
Joseph N. Pew, Jr.
William Rogers, Jr.
Frank N. Speller

1929
N. E. Bonn
Bernard Davis
Rupen Eksergian
Edward C. Haines
Malcolm Lloyd Hayward
Linn Helander

1929 (cont.)
Randal Morgan, III
Harold F. Pitcairn
Lawrence Saunders
A. Kelvin Smith
I. Melville Stein
William Stericker
Harden Franklin Taylor
Jacques L. Vauclain
Albert J. Williams, Jr.
Arthur M. Wilson, Jr.
C. T. R. Wilson
Enos E. Witmer

1930
Mildred Allen
William M. Barret
Aldus Fogelsanger
John Gardiner, Jr.
Morton Gibbons-Neff
Norman R. Gibson
Carroll Hodge
Walter J. Lehman
R. P. Long
S. B. Morehouse
William C. Peterman
G. E. Wiltbank

1931
Charles E. Berger
Carl Breer
Abraham D. Caesar

1931 (cont.)
Daniel B. Curll, Jr.
Edward Dawson
J. Bennett Hill
Frederick C. Holtz
Penrose R. Hoopes
William Melas
Parry H. Moon
Julius Neumueller
Laurence P. Sharples

1932
Arthur Fleischer
William A. Heine
Wynn Laurence LePage
Robert McLean
E. Burke Wilford

1933
Charles A. Bareuther
George E. Crofoot
George S. Gardner
Walter H. Hartung
Karl S. Howard
Edward R. Hughes
Annetta R. Masland
Ellen-Jarden Nolde
J. Livingstone Poultney
George A. Smith
Floyd T. Tyson
Wilfred H. Wickersham

The following are Gold Card Members, having belonged continuously for fifty years or more:

Fred H. Colvin '88
G. H. Clamer '91
J. H. Granberry '95
Edward Woolman '95
E. A. Muller '99
James M. Caird '01
Charles H. Howson '03
Frank S. Busser '04
C. Mahlon Kline '04
George R. Hall '05
Darthela Clark '07
Frank Shaw Clark '07
W. M. C. Kimber '08
Theobald F. Clark '09
Walton Clark, Sr. '09
James McGowan, Jr. '09
T. Edward Ross '09

LIBRARY

The Committee on Library desires to add to the collections any technical works that members may wish to contribute. Contributions will be gratefully acknowledged and placed in the Library. Duplicates received will be transferred to other libraries as gifts of the donor. 365 items have been added the past month.

Photostat service. Photostat prints of any material in the collections can be supplied on request.

The Library and reading room are open from 9 A.M. until 5 P.M. on Mondays, Tuesdays, Thursdays, Fridays and Saturdays; and 2 P.M. until 10 P.M. on Wednesdays.

RECENT ADDITIONS

AERONAUTICS

POPE, ALAN. Aerodynamics of Supersonic Flight. Ed. 2. 1958.
ZUCROW, MAURICE J. Aircraft and Missile Propulsion. Vols. 1–2. 1958.

ARCHITECTURE AND BUILDING

PARKIN, PETER HUBERT AND HUMPHREYS, HENRY ROBERT. Acoustics, Noise and Buildings. 1958.
SEVERNS, WILLIAM HARRISON AND FELLOWS, JULIAN ROBERT. Air Conditioning and Refrigeration. 1958.

ASTRONOMY

BAILY, FRANCIS. Astronomical Tables and Formulae Together with a Variety of Problems Explanatory of their Use and Application. 1827.
FERGUSON, JAMES. Astronomy Explained upon Sir Isaac Newton's Principles. Ed. 9. 1794.
HERSCHEL, JOHN FREDERICK WILLIAM. Outlines of Astronomy. 1876.
HUMBOLDT, FRIEDRICH HEINRICH ALEXANDER VON. Cosmos; a Sketch of a Physical Description of the Universe. Vols. 1–4. 1850–1852.
KLINKERFUES, ERNST FRIEDRICH WILHELM. Theoretische Astronomie. 1871.
LAPLACE, PIERRE SIMON, MARQUIS DE. The System of the World. Vols. 1–2. 1830.
LEE, THOMAS J. A Collection of Tables and Formulae Useful in Geodesy and Practical Astronomy, Including Elements for the Projection of Maps. 1849.
NARRIEN, JOHN. Practical Astronomy and Geodesy. 1845.
NEWCOMB, SIMON AND HOLDEN, EDWARD SINGLETON. Astronomy for Schools and Colleges. 1879.
OLMSTED, DENISON. A Compendium of Astronomy. Ed. 2. 1842.
PONTÉCOULANT, PHILIPPE GUSTAVE DOULCET, GRAF DE. Théorie Analytique du Systemè du Monde. Ed. 2. Vol. 1. 1856.
PONTIFICAL ACADEMY OF SCIENCE. Stellar Populations. 1958.
SCHWARZCHILD, MARTIN. Structure and Evolution of the Stars. 1958.
STOCKWELL, JOHN N. Theory of the Moon's Motion. 1881.
WHISTON, WILLIAM. Astronomical Lectures. Ed. 2. 1728.

AUTOMATIC CONTROL

COSGRIFF, ROBERT LIEN. Nonlinear Control Systems. 1958.
ECKMAN, DONALD P. Automatic Process Control. 1958.
HOLZBOCK, WERNER G. Automatic Control, Principles and Practice. 1958.
JURY, ELIAHU IBRAHIM. Sampled-Data Control Systems. 1958.
SUTHERLAND, ROBERT L. Engineering Systems Analysis. 1958.

BIOGRAPHY

BLOCHMAN, LAWRENCE GOLDTREE. Doctor Squibb; the Life and Times of a Rugged Idealist. 1958.

V.2
195

BIOLOGICAL CHEMISTRY

BIOPHYSICAL SOCIETY. 1ST SYMPOSIUM, CAMBRIDGE, MASS., 1958. Microsomal Particles and Protein Synthesis. 1958.

BOTANY

COCHRANE, VINCENT W. Physiology of Fungi. 1958.

CHEMISTRY AND CHEMICAL TECHNOLOGY

BAGNALL, K. W. Chemistry of the Rare Radioelements. 1957.
BATTISTA, O. A. Fundamentals of High Polymers. 1958.
BLUMENTHAL, WARREN B. The Chemical Behavior of Zirconium. 1958.
BOLTZ, DAVID F., ED. Colorimetric Determination of Nonmetals. 1958.
BONNAR, ROBERT U.; DIMBAT, MARTIN AND STROSS, FRED H. Number-Average Molecular Weights. 1958.
BOVEY, FRANK A. The Effects of Ionizing Radiation on Natural and Synthetic High Polymers. 1958.
COOK, ROBERT P., ED. Cholesterol. 1958.
Gas Chromatography. 1958.
GORUP VON BESANEZ, EUGEN FRANZ. Lehrbuch der Chemie für den Unterricht auf Universitäten und mit Besonderer Berücksichtigung des Standpunktes Studirender Mediciner. Vol. 1–2. 1859–60.
GUNSTONE, F. D. An Introduction to the Chemistry of Fats and Fatty Acids. 1958.
MOELLER, THERALD. Qualitative Analysis. Ed. 1. 1958.
NEILANDS, J. B. AND STUMPF, PAUL K. Outlines of Enzyme Chemistry. Ed. 2. 1958.
PENNER, S. S. Chemistry Problems in Jet Propulsion. 1957.
REID, E. EMMET. Organic Chemistry of Bivalent Sulfur. Vol. 1. 1958.
SCHWARZENBACH, GEROLD. Die Komplexometrische Titration. Ed. 3. 1957.
SOCIETY OF CHEMICAL INDUSTRY. Industrial Carbon and Graphite. 1958.

COMPUTERS

ALT, FRANZ L. Electronic Digital Computers. 1958.
KARPLUS, WALTER J. Analog Simulation. 1958.
NEUMANN, JOHANN LUDWIG VON. The Computer and the Brain. 1958.

ELECTRICITY AND ELECTRICAL ENGINEERING

CAUER, WILHELM. Synthesis of Linear Communication Networks. Ed. 2. 1958.
DUMMER, G. W. A. Fixed Resistors. 1956.
HARRINGTON, ROGER F. Introduction to Electromagnetic Engineering. 1958.
HIGONNET, RENÉ A. AND GREA, RENÉ A. Logical Design of Electrical Circuits. 1958.
RADIO-ELECTRONICS-TELEVISION MANUFACTURERS ASSOCIATION. Proceedings of the 2nd RETMA Conference on Reliable Electrical Connections, 1956. 1957.

ENGINEERING

BOYER, WALTER C. AND ABRAMS, JOEL I. Influence Lines for Continuous Beams. 1958.
DURELLI, AUGUSTO J.; PHILLIPS, E. A. AND TSAO, C. H. Introduction to the Theoretical and Experimental Analysis of Stress and Strain. 1958.
HAMMOND, ROLT. Water Power Engineering and Some Electrical Problems. 1958.
Recent Advances in the Engineering Sciences. 1958.

FOOD

ANDERSON, OSCAR EDWARD. The Health of a Nation; Harvey W. Wiley and the Fight for Pure Food. 1958.
JACOBS, MORRIS BORIS. The Chemical Analysis of Foods and Food Products. Ed. 3. 1958.

GEOLOGY

BUSK, HENRY GOULD. Earth Flexures. 1957.
GUILCHER, ANDRÉ. Coastal and Submarine Morphology. 1958.
HEINRICH, EBERHARDT WILLIAM. Mineralogy and Geology of Radioactive Raw Materials. 1958.
MASON, BRIAN. Principles of Geochemistry. Ed. 2. 1958.

HOROLOGY

ADRIEN, E. Aux Horlogers. 1888.
BEILLARD, ALFRED. La Montre. 1907.
ERIZZO, NICOLO. Relazione Storico-Critica della Torre dell 'Orologio di S. Marco in Venezia. 1860.
FOUCHER, M. P. Manuel d'Horlogerie Eleve des Fabriques de Geneve. 1850.
HESSEN, ANDRE. Memoire sur l'Horlogerie. 1784.
HILLMANN, BRUNO. Die Reparatur Komplizierter Taschenuhren. 1911.
LLOYD, H. ALAN. Some Outstanding Clocks over Seven Hundred Years 1250–1950. 1958.
SIRE, GEORGES. L'Horlogerie a l'Exposition Universelle de 1867 a Paris. 1870.

INDUSTRIAL MANAGEMENT

BARNES, RALPH MOSSER. Motion and Time Study. Ed. 4. 1958.

MANUFACTURE

APPS, E. A. Printing Ink Technology. 1958.
COLEMAN, D. C. The British Paper Industry, 1495–1860. 1958.
HERRMANN, ERHARD. Handbuch des Stranggiessens. 1958.

MATHEMATICS

ADLER, IRVING. The New Mathematics. 1958.
COURT, NATHAN ALTSHILLER. Mathematics in Fun and in Earnest. 1958.
COX, D. R. Planning Experiments. 1958.
FERGUSON, ROBERT O. AND SARGENT, LAUREN F. Linear Programming. 1958.
FORSYTHE, GEORGE ELMER AND ROSENBLOOM, PAUL C. Numerical Analysis and Partial Differential Equations. 1958.
FRANKLIN, PHILIP. An Introduction to Fourier Methods and the Laplace Transformation. 1958.
HUREWICZ, WITOLD. Lectures on Ordinary Differential Equations. 1958.
KAPLAN, WILFRED. Ordinary Differential Equations. 1958.
ONOE, MORIO. Tables of Modified Quotients of Bessel Functions of the First Kind for Real and Imaginary Arguments. 1958.
PAGE, CHESTER HALL. Algebra of Electronics. 1958.
RICHMOND, A. E. Calculus for Electronics. 1958.
SOKOLNIKOFF, IVAN STEPHEN AND REDHEFFER, R. M. Mathematics of Physics and Modern Engineering. 1958.
Some Aspects of Analysis and Probability. 1958.
TAYLOR, ANGUS ELLIS. Introduction to Functional Analysis. 1958.
WALLACE, ANDREW H. Homology Theory on Algebraic Varieties. 1958.

MECHANICAL ENGINEERING

HRYNISZAK, W. Heat Exchangers; Applications to Gas Turbines. 1958.
INSTITUTION OF MECHANICAL ENGINEERS. Proceedings of the Conference on Lubrication and Wear. 1958.

METALLURGY

CONFERENCE ON THE PHYSICAL CHEMISTRY OF IRON AND STEELMAKING. The Physical Chemistry of Steelmaking; Proceedings. 1958.

V.2
195

The Metal Molybdenum. 1958.
NEW JERSEY ZINC CO. Zinc Oxide Rediscovered. 1957.

METEOROLOGY

BATES, DAVID ROBERT. Earth and its Atmosphere. 1958.
DEFANT, ALBERT. Ebb and Flow; the Tides of Earth, Air and Water. 1958.

MINING ENGINEERING

Progress in Mineral Dressing. 1958.

MISSILES AND ROCKETS

BÜDELER, WERNER. Operation Vanguard. 1958.
DOW, RICHARD B. Fundamentals of Advanced Missiles. 1958.
HALEY, ANDREW GALLAGHER. Rocketry and Space Exploration. 1958.
SPECIAL COMMITTEE OF THE INTERNATIONAL GEOPHYSICAL YEAR. Annals of the International Geophysical Year. 1958.
U. S. AIR FORCE. The United States Air Force Report on the Ballistic Missile. 1958.

NUCLEAR ENGINEERING

Elsevier's Dictionary of Nuclear Science and Technology, in Six Languages: English/American, French, Spanish, Italian, Dutch, and German. 1958.
HAUSNER, HENRY H. Powder Metallurgy in Nuclear Engineering. 1958.
STEPHENSON, RICHARD. Introduction to Nuclear Engineering. Ed. 2. 1958.

OPTICS

BOLL, R. H. AND OTHERS. Tables of Light-Scattering Functions Relative Indices of Less than Unity and Infinity. 1958.
GRAY, PETER. Handbook of Basic Microtechnique. Ed. 2. 1958.
HALE, ARTHUR J. Interference Microscope in Biological Research. 1958.
SMITH, SIGMUND L. Ore Microscopy. Ed. 2. 1957.

PETROLEUM TECHNOLOGY

BROOKS, BENJAMIN TALBOTT AND OTHERS, ED. The Chemistry of Petroleum Hydrocarbons. 1954–55.

PHOTOGRAPHY

ALLEN, ROY MORRIS. Photomicrography. Ed 2. 1958.
BAINES, H. The Science of Photography. 1958.
SIPLEY, LOUIS WALTON. Photomechanical Halftone. 1958.

PHYSICS

CHISHOLM, J. S. R. AND BORDE, A. H. DE. An Introduction to Statistical Mechanics. 1958.
DUNGEY, J. W. Cosmic Electrodynamics. 1958.
ELFRON, ALEXANDER. Mechanics. 1958.
FRÖHLICH, HERBERT. Theory of Dielectrics; Dielectric Constant and Dielectric Loss. Ed. 2. 1958.
JACKSON, J. D. The Physics of Elementary Particles. 1958.
LAPLACE, PIERRE SIMON, MARQUIS DE. A Treatise upon Analytical Mechanics. 1814.
Nuclear Masses and their Determination. 1957.
SINNOTT, MAURICE J. The Solid State for Engineers. 1958.
STEPHENSON, G. AND KILMISTER, C. W. Special Relativity for Physicists. 1958.
TEMPLE, G. An Introduction to Fluid Dynamics. 1958.
THIRRING, WALTER E. Principles of Quantum Electrodynamics. 1958.

PROGRAMMING

GASS, SAUL I. Linear Programming: Methods and Applications. 1958.
METZGER, ROBERT W. Elementary Mathematical Programming. 1958.
VAZSONYI, ANDREW. Scientific Programming in Business and Industry. 1958.

SANITARY ENGINEERING

BABBITT, HAROLD E. AND BAUMANN, E. ROBERT. Sewerage and Sewage Treatment. Ed. 8. 1958.
McCABE, JOSEPH AND ECKENFELDER, W. W., ED. Biological Treatment of Sewage and Industrial Wastes. Vol. 1–2. 1956–58.

SCIENCE

HANSON, NORWOOD RUSSELL. Patterns of Discovery. 1958.
SCHWARTZ, GEORGE I. AND BISHOP, PHILIP W., ED. Moments of Discovery. 1958.

SCIENTIFIC INSTRUMENTS

ADLER, IRVING. The Tools of Science; from Yardstick to Cyclotron. 1958.

STATISTICS

GUMBEL, EMIL JULIUS. Statistics of Extremes. 1958.
HAGGARD, ERNEST A. Intraclass Correlation with the Analysis of Variance. 1958.

WOOD

VORREITER, LEOPOLD. Holztechnologisches Handbuch. 1949–58.

V.2
195

DO YOU KNOW OF THE FRANKLIN INSTITUTE'S NEED FOR FINANCIAL SUPPORT

Since 1824 The Franklin Institute, through wise and conservative management, has been partially self-supporting.

As an old institution, established in the public interest, The Franklin Institute has tried to earn most of its cost by diligent and productive work. Like many other institutions of a non-profit nature, The Institute has for many years found it increasingly difficult to perform the broad educational services of which the growing nation and territories are ever in need

The educational service rendered by The Institute begins with the early grades of our elementary schools and continues throughout an individual's professional and industrial career. This period represents a span of fifty years.

Despite an erroneous public impression gained, perhaps, by the excellence and wide range of services performed, that it is a wealthy, richly endowed organization, The Institute always needs additional funds to help it perform its broad educational program.

There is a warm satisfaction in giving financial support to an organization that will use it constructively to help advance and improve our type of civilization.

Your gift or bequest, large or small, will be deeply appreciated. We shall be pleased to give any additional information regarding gifts or memorials.

Where property is transferred, title should be in the name of The Franklin Institute of the State of Pennsylvania for the Promotion of the Mechanic Arts.

Will you please write to: The Secretary, The Franklin Institute, Benjamin Franklin Parkway at Twentieth Street, Philadelphia 3, Pennsylvania, for any additional information.

BOOK REVIEWS

MATHEMATICAL THEORY OF COMPRESSIBLE FLUID FLOW, by Richard von Mises, completed by Hilda Geiringer and G. S. S. Ludford. 514 pages, diagrams, 6 × 9 in. New York, Academic Press Inc., 1958. Price, $15.00.

It is no mean task to combine rigorous analysis with easy readability in presenting the mathematical theory of compressible fluid flow. This has been successfully achieved in this book. The first three chapters, written by the late Professor Richard von Mises before his death, provide the keynote for the rest of the book which was completed by his wife, Hilda Geiringer, together with G. S. S. Ludford.

In Chapter I, the basic differential equations of fluid flow in three dimensions are carefully derived in a completely general manner, including the effects of viscosity and heat conduction. The origin and necessity of each equation is pointed out, together with its implications, thus laying a solid foundation for the superstructure of the mathematical theory of compressible fluid flow. The underlying assumptions are examined, as for example, that of a perfect gas, and in addition it is shown how a non-perfect gas can be treated analytically. The author uses the novel concept of a specifying equation which clarifies the role of thermodynamics in the mechanics of compressible fluids.

The mathematical analysis is thorough, yet simply presented, and no intervening steps in any derivation are omitted on the assumption that they are obvious to the reader. The author carefully paves the way for the introduction of vector notation and the use of integral theorems in a manner that will be appreciated by the student who is barely acquainted with these subjects. A typical example will be found in Article 6.1. Here the author derives Stokes theorem in vector notation before introducing the Vortex Theory of Helmholtz and Kelvin. Of all the different derivations of Stokes theorem that this reviewer has seen, not one surpasses this for clarity and simplicity.

Small perturbation theory, which plays an important role in aerodynamics is not considered further in this book after Article 4 in the first chapter. It was the author's intention to discuss extensively the approximation theories in the second part of his work; this, unfortunately, he did not live to do.

The general theorems of vorticity and irrotational motion are presented in Chapter II, along with the relationships of steady flow. Two noteworthy features of this chapter are the thorough, yet lucid, treatment of the hodograph representations and the method of characteristics.

The third chapter specializes the general equations previously described to those of one dimensional flow. Solutions are given for flow with viscosity and heat conduction and of the non-steady flow of an ideal fluid. Examples of simple waves and the theory of shock phenomena bring this chapter to a close, and with it, the work of Richard von Mises.

The last two chapters were written by the co-authors of the book. The further development of the theory of plane steady potential flow is to be found in Chapter IV, which was written by Hilda Geiringer, who also wrote the text on the development of Chaplygin's Method and the article on Transonic Flow in Chapter V. The bulk of Chapter V is an excellent treatment of shock theory and was written by G. S. S. Ludford. The clarity of presentation combined with thoroughness of analysis which characterizes the first three chapters is also present in the last two. As a matter of fact, the smoothness of style uniformly present throughout the book leads one to suspect that the co-authors played a large part in achieving this.

The book was written as an advanced textbook for both graduate students and research workers. Its complete lack of exercises for the student prevent one from prescribing it as a classroom text, but its other qualities make it indispensable to the student who wishes to gain deeper insight into the mathematical theory of compressible flow. The research

worker will find this book a valuable addition to his library. The practising gas dynamicists who had their formal training in engineering schools will not find themselves overwhelmed by the mathematics in this book; those who entered the field of gas dynamics after completing their education in physics or mathematics will find all the mathematical exactitude they desire.

ARTHUR A. EZRA
The Martin Company

VACUUM METALLURGY, edited by R. F. Bunshah. 472 pages, illustrations, 6 × 9 in. New York, Reinhold Publishing Corp., 1958. Price, $12.50.

This book consists of a series of 28 lectures delivered at the Department of Metallurgical Engineering of the New York University, College of Engineering in June, 1957. It is to be the first in a new series on Materials Technology. The book comes at a time when vacuum metallurgy is of considerable interest in the solution of problems involving pure metals and alloys. There have been great changes in this field in the last ten years. Unfortunately, there are still a great number of researchers who have not followed the technology and who still use vacuum techniques that they used in school. This book should be of great value to bring them, as well as others, up to date in this fast moving field.

It is difficult to collect the individual lectures of a group of men into one text and still maintain a balanced coordinated coverage of the subject. Dr. Bunshah has done a creditable job in this respect. The format is logical and the coverage excellent. The 28 lectures are proportioned into ten parts dealing with vacuum equipment, thermodynamics and kinetics, arc melting, induction melting, electron bombardment melting, degassing, distillation, applications, analytical techniques, and future trends.

The section on applications occupies about a fifth of the text. It covers current practice in specified areas and also gives comparison data for materials treated in vacuo and in gas atmospheres. Subjects discussed are ferrous base and high temperature alloys, refractory metals, nuclear power plant materials, electronic materials, powder metallurgical products, and vacuum coatings for metals. This section enables the reader to see what some of the advantages of vacuum processing are and gives him an insight into its potentialities.

Three chapters are devoted to thermodynamics and kinetics. One of these is somewhat elementary in covering very briefly such things as the Phase Rule, LeChatlier's Principle, the Gas Laws of Thermodynamics, etc. Also in another of these three chapters the figures are poorly reproduced. In general, however, this part of the text is useful.

The chapter devoted to electron bombardment melting techniques is somewhat disappointing. It is written in such a general way that it is of very little practical value except to the person almost completely unfamiliar with the technique. A minor oversight is the lack of captions for some of the figures.

Not all of the chapters contain references; however, the editor has compiled a rather complete and useful bibliography to supplement the text references. There are author and subject indexes.

R. L. SMITH
The Franklin Institute Laboratories

ANALYSIS AND CONTROL OF NONLINEAR SYSTEMS, by Y. H. Ku. 360 pages, diagrams, 6 × 9 in. New York, The Ronald Press Co., 1958. Price, $10.00.

This book is an outgrowth of a graduate course in nonlinear circuit analysis given at the Moore School of Electrical Engineering of the University of Pennsylvania by Professor Ku.

With the dawn of automation thundering all around us it becomes difficult to make a wise decision as to which books will be significant additions to one's technical library and not just some more clutter. Professor Ku's book is such a significant addition.

Ever since the installation in the early fifties of Typhoon, the tremendous analog computer at the Naval Air Development Center, and smaller analog computers elsewhere, the phase-plane analysis has been tremendously useful in presenting analog or actual equipment results.

In Professor Ku's book a new approach has been developed based on the author's method of space trajectory in n dimensions which extends the phase-plane method to phase space. This is essentially a multidimensional plot allowing solution of higher order nonlinear differential equations than the second.

For the first time we have a book which provides a general and powerful method of studying the behavior of physical systems with many degrees of freedom. The method of simultaneous phase-plane equations demonstrates that a physical system with nonlinearities anywhere and with any degree of complication can be treated in a comprehensive manner. This method is a basic apprcach which extends nonlinear analysis to feedback systems with nonlinearities. Chapter 11 on analysis of nonlinear servomechanisms and Chapter 12 on nonlinear control of feedback systems are devoted to this new field of study.

The preceding ten chapters carefully prepare the reader for the trenchant final chapters. Both analytical and topological methods of solving nonlinear differential equations are presented. Physical examples in both mechanical and electrical systems which involve nonlinearities are worked out in detail. There is a particularly intriguing example in nuclear reactor kinetics at the end of Chapter 9 which is an analysis of high order nonlinear systems. Chapter 10 presents an analysis of multi-loop nonlinear systems and discusses the method of simultaneous phase-plane equations. This is the last stage of preparation for the final chapters. To aid the reader in acquiring technical dexterity ten well chosen examples are given at the end of each chapter for the reader to solve.

After a leisurely and delightful journey through the ten chapters (delightful because of the beauty and simplicity of presentation), the reader is ready to partake of the *pièce de résistance* of the final chapters. In the chapter on analysis of nonlinear servomechanisms Professor Ku discusses responses in linear servomechanisms, nonlinear elements for improving servo performance, contactor servomechanisms, dual mode operation of nonlinear servomechanisms, multiple mode operation in a high order system, stability criterion for contactor servomechanisms, back lash in servomechanisms and nonlinear control systems for wide range input signals.

In the final chapter he discusses the theory of nonlinear control of feedback systems, systems with nonlinear control in the feedback branch, nonlinear feedback control systems with third and higher order transfer functions, systems with nonlinear control in the forward branch, nonlinear forward-control system with integral feedback, nonlinear forward-control system with derivative feedback, feedback system with two nonlinear control functions, feedback system with two linear networks and two nonlinear control networks, nonlinear feedback control to improve transient response of a system, nonlinear control in a torpedo system, stability study of higher order nonlinear control systems and applications of digital and analog computers in the design of nonlinear control systems.

In addition to writing an invaluable text, Professor Ku has compiled a remarkably complete bibliography extending from 1860 to 1958. This bibliography completes the book.

EDWARD A. KNOBELAUCH
Burroughs Corporation Research Center

SOLID STATE PHYSICS, VOLUME 7, edited by F. Seitz and D. Turnbull. 525 pages, diagrams, 6 × 9 in. New York, Academic Press Inc., 1958. Price, $12.00.

The seventh volume of the SSP series maintains the high standards of its predecessors, in the choice of topics and the competence of the treatments. We review successively the various subjects dealt with in this volume.

1. Thermal Conductivity and Lattice Vibrations Modes (pp. 1–99) P. G. Clemens

After a brief introduction to this important subject, the author devotes about a third of his exposé to an excellent presentation of the necessary background, namely the theory of quantized lattice waves, normal modes, the various types of interactions and to the approximate solution of Boltzmann's transport equation. He then treats successively the thermal conductivity of (a) *Non-Metals* (at high and low temperatures, imperfections, size effect etc.) and of (b) *Metals, Alloys and Semiconductors* (lattice and electronic components and their separation etc. . . .). This presentation exhibits the same qualities of clarity and order, shown by the author in his earlier monograph on a similar subject (on Low Temperature Thermal Conductivity, Handbuch der Physik, Vol. 14, Berlin 1956).

2. Electron Energy Bands in Solids (pp. 100–209) J. Callaway

This is a central and difficult problem of Solid State Physics, and it will remain so for many years to come. J. Reitz in SSP Vol. 1 and T. O. Woodruff in Vol. 4 have already dealt with the fundamentals of the subjects.

J. Callaway after a fifteen page critical summary of the general theory, discusses successively the alkali metals, the metals of groups II and III, the group IV elements (and related semiconductors), the transition metals and the 4 other substances. This monograph is remarkable by the wealth and scope of the information provided, and is a must for anyone interested in the energy band theory of solids.

3. The Elastic Constants of Crystals (pp. 214–352) H. B. Huntington

The classical theory of elastic constants is introduced along with the atomistic theories. An exposé of the various experimental methods is followed by an excellent and most useful set of tables of measured elastic constants, of various metal groups, rare gas solids, ferromagnetic materials etc. The last part is a lucid and thorough discussion of the dependence of elastic constants on Temperature, Pressure, Composition Phase Changes and Relaxation Phenomena.

4. Wave Packets and Transport of Electrons in Metals (pp. 353–378) H. W. Lewis

After a brief restatement of the current theory of electronic transport, the author analyzes some of its shortcomings and their consequences. Emphasis is put on the unadiabatic nature of the scattering processes in metals.

5. Study of Surfaces by Using New Tools (pp. 379–425) J. A. Becker

With the growing importance of the physics of surface phenomena, Becker's presentation of three new and powerful experimental tools of surface investigation will be welcomed by many physicists. The three tools are the ion gauge, the FEM (field emission microscope) and the FIM (field ion microscope). The ion gauge measures the rates of adsorption and desorption, the FEM yields the dependence of the work function on the crystallographic planes and the FIM allows the location of individual atoms on metal surfaces.

6. The Structures of Crystals (pp. 426–503) A. F. Wells

This is an illuminating and up-to-date survey. The author is to be commended for the clarity of his exposé and especially for the excellent diagrams and tables. It is certain that this article will be frequently and profitably consulted by many physicists and chemists.

HENRI AMAR
The Franklin Institute Laboratories

ROCKET PROPELLANTS, by Francis A. Warren. 218 pages, illustrations, 6 × 9 in. New York, Reinhold Publishing Corp., 1958. Price, $6.50.

With the coming of age of astronautics many books have appeared on satellites and space flight. In most of these some bits of information have been given concerning propulsion systems which permit the payloads to go into orbit or beyond the Earth's gravitational field. In these books we may find references to liquid and solid propellants, to rocket motors, to pumps, to igniters but always the treatment is meager almost to the point of frustration.

Now appears *Rocket Propellants* written by Francis A. Warren who, in working for the Southwest Research Institute, coordinates research on propellants and their combustion. From an excellent background in propellants he has put together a fascinating story on why rockets work. The author claims this is written ". . . to provide technical men with basic information on the materials being used to propel the rockets and missiles of today, ..." The author has capably fulfilled his commitment not only to the technical personnel but also to those non-technical people who find propellants absorbing and would like to know about them.

In the literature we find many references to the various types of propellants, the grain shapes typical of the state of the art today, the ingredients of both the solid and liquid propellants, the processing the "pros" use in producing these fuels and the performance characteristics of propellants. Here for the first time we find this material collated in a book.

When we watch a big rocket being launched and see the plume of fire roaring down on the deflector little does the layman realize the tremendous volume of research which has been successfully carried through to make possible the precise burning of the propellants. Chapter V, The Burning of Propellants, is a classic treatment of what happens when the rocket is ignited. Temperature, burning rate, velocity of exhaust are some of the topics discussed in this chapter. The author in comparatively

V.2
195

few pages reveals much of the burning process.

Ignition and igniters are given a chapter. This is one rarely mentioned in conventional books yet this reviewer finds it one of the most fascinating. Extreme ingenuity has been exercised by designers to insure the ignition of the rocket. This chapter shows what must be done to realize the burning state.

The author concludes with chapters on solid and liquid propellants, the important element of safety in manufacturing and handling propellants and finally there is a projection into the future.

The author has put together a readable and useful book which will be much in demand in the engineer's library. This book was long overdue and it may well set the pattern for others to follow.

I. M. LEVITT
The Franklin Institute, Planetarium

PUBLICATIONS RECEIVED

THEORY OF ELLIPTIC FUNCTIONS, by Harris Hancock. Unabridged and unaltered republication of the first edition. 498 pages, 5⅜ × 8½ in. New York, Dover Publications, 1959. Price, $2.55 (paper).

ELLIPTIC INTEGRALS, by Harris Hancock. Unabridged and unaltered republication of the first edition. 104 pages, diagrams, 5⅜ × 8½ in. New York, Dover Publications, Inc., 1959. Price, $1.25 (paper).

THE ELEMENTS OF NON-EUCLIDEAN GEOMETRY, by D. M. Y. Sommerville. Unabridged and unaltered republication of the first edition. 274 pages, diagrams, 5⅜ × 8½ in. New York, Dover Publications, Inc., 1959. Price, $1.50 (paper).

THE FOUNDATIONS OF EUCLIDEAN GEOMETRY, by Henry George Forder. Unabridged and unaltered republication of the first edition. 349 pages, diagrams, 5⅜ × 8½ in. New York, Dover Publications, Inc., 1959. Price, $2.00 (paper).

THE THEORY OF THE POTENTIAL, by William Duncan MacMillan. Unabridged and unaltered republication of the first edition. 469 pages, diagrams, 5⅜ × 8½ in. New York, Dover Publications, Inc., 1959. Price, $2.25 (paper).

AN INTRODUCTION TO THE GEOMETRY OF *N* DIMENSIONS, by D. M. Y. Sommerville. Unabridged and unaltered republication of the first edition. 196 pages, diagrams, 5⅜ × 8½ in. New York, Dover Publications, Inc., 1959. Price, $1.50 (paper).

THE GENETICAL THEORY OF NATURAL SELECTION, by Ronald A. Fisher. Second revised edition of the work first published in 1929. 291 pages, diagrams, 5⅜ × 8 in. New York, Dover Publications, Inc., 1959. Price, $1.85 (paper).

ELASTICITY, PLASTICITY & STRUCTURE OF MATTER, by R. Houwink. Unabridged republication of the second edition. 368 pages, diagrams, 5⅜ × 8 in. New York, Dover Publications, Inc., 1959. Price, $2.45 (paper).

THE THEORY OF THE PROPERTIES OF METALS AND ALLOYS, by N. F. Mott and H. Jones. Reprinted from corrected sheets of the first edition. 326 pages, diagrams, 5⅜ × 8½ in. New York, Dover Publications, Inc., 1959. Price, $1.85 (paper).

STUDIES ON THE STRUCTURE AND DEVELOPMENT OF VERTEBRATES, by Edwin S. Goodrich, Two-volume unabridged and unaltered republication of the one-volume first edition. 837 pages, diagrams, 5¼ × 8 in. New York, Dover Publications, Inc., 1959. Price for each volume, $2.50 (paper).

GUIDE TO THE LITERATURE OF MATHEMATICS AND PHYSICS INCLUDING RELATED WORKS ON ENGINEERING SCIENCE, by Nathan Grier Parke III. Revised and expanded version of the first edition. 436 pages, 5⅜ × 8 in. New York, Dover Publications, Inc., 1958. Price, 2.49_4$(paper).

CURRENT TOPICS

New Powder Pattern Technique.—A new method for delineating the domain structure at the surfaces of ferroelectric crystals was described recently in a paper presented to the American Physical Society by G. L. Pearson and W. L. Feldmann of Bell Telephone Laboratories. It has been used to delineate domain structures in great detail on a wide variety of crystals in which domains have never been observed before.

According to its discoverers, the method should be applicable to the study of piezoelectric and pyroelectric charged surfaces as well as ferroelectric materials.

The new technique uses colloidal suspensions of electrostatically charged powders in an insulating organic liquid. When a few drops of this suspension are applied to the face of the crystal, the charged powder is immediately attracted to the ferroelectric domains carrying an opposite charge, and covers their entire area.

The most effective materials for this work are commercial spray-grade sulfur and red lead oxide, each suspended in hexane. The sulfur deposits on negatively charged domains, while the lead oxide deposits on the positively charged domains. Each of the suspensions is applied separately; the second is not applied until the hexane in the first has evaporated. If the two suspensions mix on the crystal surface, each may lose its charge. In this event, no pattern is formed. The powders are fixed in place indefinitely by their electrostatic charge after the hexane evaporates.

The yellow sulfur and red lead oxide provide brightly colored delineation of the positive and negative domains, and the pattern shows great detail.

A dispersion of a cross linked polymer derived from polystyrene can also be used as the negatively charged colloid, in place of the lead oxide. This can be dyed any desired color with an oil soluble dye.

The basis for the success of the new technique lies in the fact that although the colloid as a whole is electrically neutral, individual particles acquire a diffuse, double-layer charge when brought in contact with the liquid. Under the influence of the "built-in" electric field, the colloidal particles are attracted either to the positive or negative domains depending on the orientation of their dipole layers. For these experiments, an insulating liquid of low viscosity and low dielectric constant such as hexane is desirable, so that the charged particles are free to move toward the ferroelectric domains under maximum electrostatic attraction.

Powder patterns of an entirely different nature result if a colloid of finely divided barium titanate in hexane is used instead of sulfur and lead oxide. The $BaTiO_3$ particles carry no net electric charge, but they do have a very high dielectric constant. Thus, when they are placed on the surface of a ferroelectric crystal containing positive and negative domains, the particles polarize in the external electrostatic fields and are deposited at domain boundaries where large field gradients exist. The resulting powder patterns outline the domain boundaries well, but do not differentiate between positively and negatively charged domains.

This new technique has provided the first information available on the do-

V.2(
195

main structure of a number of crystalline ferroelectric materials, including triglycine sulfate and guanidinium gallium selenate hexahydrate. Previous optical determinations which have been made on Rochelle salt, and domain etching procedures on barium titanate have been confirmed by the new method also.

Thus, a simple, easily employed technique joins the group of tools available to the physical chemist and physicist in their continuing search for knowledge of the ultimate structure of matter.

The Proceedings of the Royal Institution of Great Britain.—The *Proceedings of the Royal Institution* are now being published three times a year instead of annually. The *Proceedings* contain accounts of the well-known Friday Evening Discourses and one advantage of the new procedure will be that the Discourses will appear in print soon after their delivery.

The Evening Discourses at the Royal Institution were started by Michael Faraday in 1826 and for over 130 years they have maintained the highest standards of popular exposition. The Discourses are famous, not only because they are given by leading men of science, but also because it is traditional to illustrate the subject by experiments and demonstrations whenever possible.

The *Proceedings* therefore contain authoritative accounts of research and learning, written for the non-specialist and covering many branches of science and other subjects. In these days of specialization, such accounts enable the reader to get a broad survey of the most important advances in a wide field.

Moisture Balance with Built-in Autotransformer.—A new and improved moisture balance for fast and highly accurate determinations of moisture content in a wide variety of materials has been designed by Central Scientific Company, Chicago. Principal feature of the new model is its built-in autotransformer which regulates voltage automatically and provides more convenient temperature control than previous moisture balances in which the autotransformer was a separate unit.

Among the materials for which the balance may be used with a high degree of accuracy and reliability are: nonfat milk powder, dry milk, soybean products, pharmaceuticals, chemicals, corn products, leather, fiber, latex, paper pulp, soap and detergents, food products, ceramic powder, clays, resins, paint pigments, soil, raw meat, fertilizer, dextran, yeast, plastics, lactose, plant seeds, and cotton. Products that do not change their chemical structure or decompose while losing water are most suitable for testing.

Simple to operate by even an inexperienced laboratory technician, the moisture balance is capable of reducing from one-half hour, or more, to only a few minutes the time required for accurately testing the moisture content of a material.

According to Central Scientific, the balance performs both drying and weighing operations simultaneously, thus eliminating time-consuming weighing of samples on an analytical balance, with subsequent drying in a vacuum oven and then reweighing.

To operate the Cenco moisture balance, a 5-gram sample (exact weight need not be known) is placed in the balance pan and the indicator crank is set for 100 per cent moisture. The hood is then lowered, the lamp switch turned on, and the infrared heat quickly penetrates deeply into the sample. A few minutes later, with moisture driven off, the percent of moisture lost is read

directly on an easy-to-read calibrated scale.

The improved unit also comes equipped with disposable weighing dishes, made deeper than former models. These provide a better flexibility of loads and enable the operator to use larger liquid samples, or bulkier dry samples. The dishes are ridged to keep liquid samples uniformly distributed in the weighing pan and eliminate spillage.

The built-in magnetic damper reduces pan vibrations and speeds weighings. An extra torsion wire for 25 gram samples is supplied for handling heavier loads.

The new Cenco moisture balance is housed in a completely redesigned and compact case of solid cast aluminum with Cenco blue wrinkle enamel. It can be used wherever a 115-volt, 60 cycle outlet is available.

In-Circuit Transistor Tester.—The first transistor tester capable of checking the performance of transistors while they are connected within their circuits, has been developed by Philco Corporation, and a commercial model will be available in the near future. In-circuit transistor testing is extremely important since the method saves trouble shooting and servicing time without turning on power in the equipment.

Other commercially available transistor testers cannot perform in-circuit transistor measurements since they are unable to differentiate between normal input and output signals generated by the transistor and spurious signals appearing at either the input or output terminals. These spurious signals arise from the sneak paths propagated by the circuitry surrounding the transistor under test.

Low impedance methods are employed in both the input and output circuits to nullify the effects of the external circuitry.

Cathode Follower Probe Improves Accelerometer Performance.—A new type of Cathode Follower Probe, requiring no separate power, has been developed by Columbia Research Laboratories. Composed entirely of passive circuitry, this new device provides an improved solution to the problem of using long cables up to 100 feet or more without loss of accelerometer sensitivity.

Basically, the device functions as the first stage of the Cathode Follower and because of its small size and light weight ($\frac{3}{4} \times \frac{1}{2}$-in. diameter and $\frac{3}{4}$ oz.) the unit can be mounted close to the accelerometer. This has the effect of bringing the Cathode Follower out to the transducer. In low g-level studies this affords the possibility of using very short low-noise cable going into the probe, thereby providing a means of increasing sensitivity as much as four times with some accelerometers.

The Probe connects directly to the input jack of the Cathode Follower and requires no circuit adjustment to install. It is detachable, extremely small and rugged, free from microphonics and capable of withstanding temperatures up to 600° F.

Acoustoelectric Effect in Germanium.—A direct current can be induced in a semiconductor under certain conditions by passing acoustic waves through it. This effect, which has been studied extensively by Gabriel Weinreich of Bell Telephone Laboratories, is known as the "acoustoelectric effect."

An acoustic wave traveling through a semiconductor tends to produce a net force acting on the charge carriers in the direction of propagation of the wave. To offset this force, an electric

field is induced in the semiconductor material, and this field can be measured by attaching contacts along the length of the sample.

Since this effect depends on some bunching of the carriers, it is normally reduced greatly by their mutual electrostatic repulsion. There are some situations, however, in which more than one type of carrier is present, and it is possible to bunch each type separately without developing a net space charge. Such is the case with *n*-type germanium, in which the electrons belong to a band which has a number of distinct energy minima or "valleys." The electrons in the vicinity of these various valleys react differently to the acoustic wave, giving rise to the acoustoelectric effect. The magnitude of this effect gives a measure of the intervalley scattering time, that is, the mean transition time between the separate groups of states in the conduction bands which lie near the minima of energy (valleys).

Experimental verification of the acoustoelectric effect has been obtained by passing acoustic waves at frequencies of 20 mc. and 60 mc. through a bar of *n*-type germanium, and measuring the voltage induced along the bar. To minimize stray effects, the acoustic waves are modulated with an audio frequency, thus producing an audio frequency induced voltage rather than a d-c. voltage.

A study of intervalley scattering time has led to a better understanding of semiconductor materials. It has been found that this scattering is due in part to phonon scattering and in part to impurity scattering. These two effects may be separated, as the phonon effect becomes greater at higher temperatures (above 100° K.) while the impurity effect is predominant at temperatures below about 60° K. Between 60° K. and 100° K., the two effects are mixed.

Ferroelectric Polarization Reversal in Barium Titanate.—Recent experiments on single crystal barium titanate have demonstrated for the first time that complete ferroelectric polarization reversal can be accomplished under an applied electric field, with a single expanding domain which grows through extensive sidewise motion of the 180° domain walls. These experiments were described in a paper by Robert C. Miller of Bell Telephone Laboratories, which was presented to the Conference on the Physics of Dielectrics at Moscow.

Very little work has been reported previously on sidewise motion of 180° domain-walls in ferroelectrics. These 180° domain-walls are the boundaries between two adjacent areas or domains of opposite polarization. Sidewise motion involves the movement of boundaries in a direction perpendicular to the dipole moment of the domain. In Dr. Miller's work, a single crystal of $BaTiO_3$ is mounted with liquid electrodes applied to either side, and is subjected to an external applied field. The electrodes used were silver or platinum rods 1.0 mm. in diameter, with a small hole drilled in one end. An aqueous lithium chloride solution, saturated at room temperature, was placed in the hole as the electrolyte.

Partially switched crystals were studied by removing them from the apparatus and etching them for a short time in weak hydrofluoric acid. The positive dipole ends etch preferentially; examination with a microscope after etching allows one to observe the domains visually.

With the liquid electroded crystals, the number and size of the reversed domains in the partially switched crys-

tals was of great interest. In numerous cases, a single reversed domain comparable in size to the total electrode area was observed. Many of the domains appeared to nucleate at obvious crystalline imperfections.

In a further refinement of the technique, Miller took advantage of this nucleation phenomonon by "manufacturing" a nucleation site. This site was a sandblasted dimple about one-third the crystal thickness deep, and with a diameter about one-fourth that of the electrode.

When a dimpled sample is placed in the liquid electrode holder, nucleation of reversed domains is most probable in the dimpled region because it is subjected to a high field compared to that of the surrounding area. Once a nucleation has occurred in the dimpled region, the domain grows out from the dimple through sidewise wall motion. The single domain is roughly square, as has been shown by successive etching of the partially switched crystal. In this way, complete reversal of polarization has been accomplished for the first time with a single expanding domain, starting from a predetermined point on the crystal.

There is some evidence to indicate that impurities have an effect on the velocity of the domain wall motion, but the evidence is meager. The experiments performed here indicate that the velocity is given by the equation:

$$v = v_\infty e^{\beta/E}$$

for over three decades of velocity. The velocity for the field $E = \infty$ is v_∞, and is of the order of 10 cm/sec. The activation field varies from 2000 to 4000 v/cm.

It appears that under these conditions, this polarization reversal is analogous to magnetization reversal in some ferromagnetic materials.

Television System for High Altitude Solar Observation.—A special television system that will permit astronomers on the ground to aim and focus a telescope suspended from a balloon fifteen miles above the Earth is being developed by scientists of the Radio Corporation of America. The television equipment, comprising a specially designed slow-scanning airborne camera and transmitter as well as a ground monitoring system, is to be used in high-altitude solar observation by a Princeton University team under Dr. Martin Schwarzschild of the Department of Astronomy.

In the experiments, scheduled for next summer from a base in Minnesota, a 12-in. reflecting telescope, known as the "Stratoscope," will be carried to altitudes of 80,000 ft. for observation of the sun's surface. At these altitudes, observations may be made with little or no interference from the Earth's atomosphere, whose density and turbulence limit clear viewing from ground observatories.

The special RCA television camera will be mounted on the "Stratoscope" and linked optically with a motion picture camera that obtains a permanent photographic record of the images appearing in the 12-in. reflector. Through the airborne transmitter, also mounted on the telescope structure, the television camera will transmit to the ground a second-by-second view of what the motion picture camera sees. Watching the results on television monitor screens, the astronomers at the ground base will control the aim and focus of the telescope by means of a remote control system that also is being developed for the project.

The "Stratoscope" program, initiated and directed by Dr. Schwarzschild, produced a number of clear and detailed views of the solar surface during two unmanned flights in 1957. At

that time, however, the system did not include television and remote control equipment to keep the telescope in proper focus and aimed directly at the sun at all times. As a result, only a portion of the photographic record made by the motion picture camera provided the desired information. According to Dr. Schwarzschild, the development of the new television and control systems should result in full control of the "Stratoscope" throughout its flight, producing a complete photographic record of useful information for the astronomers.

The special RCA television system, being developed under the supervision of Dr. V. K. Zworykin, Honorary Vice President of RCA, is designed to pick up and transmit to the ground one picture per second up to a range of 150 miles. One picture per second will provide all of the information needed by the astronomers for control purposes, and will at the same time permit the use of low power equipment transmitting over a far narrower bandwidth than that required for conventional television broadcasting.

The special television camera, which will be mounted beside the motion picture camera on the telescope structure, employs a 1-in. RCA Vidicon pickup tube and transistorized circuits. Measuring only 8 × 6 × 5 in., it will be surrounded by a pressurized case for high altitude operation. The compact frequency-modulation (FM) transmitter, together with its battery power supply, also will be contained in a pressurized case. A third element in the airborne system is a special antenna arrangement contained in a shock-resistant foam package suspended below the telescope. The antennas will send television and telemetering signals to the ground station and will receive from the ground the control signals for the focusing and aiming devices.

The television camera will be linked optically to the motion picture camera by a mirror system. In operation, a shutter arrangement will cause the telescope image to be reflected briefly once per second to the television camera, which will transmit to the ground during the remainder of the second a picture identical to that recorded at the same instant by the film camera.

The ground equipment will include a television receiver and three monitors, one of which will be used for photographing the transmitted images for later checking against the permanent film record. The entire television system will operate at a frequency of about 225 megacycles, in the ultra-high-frequency (UHF) band, on a bandwidth of 200 kilocycles.

New Design for School Laboratories.—Fifteen seconds after the flip of a switch, a physics classroom laboratory was converted to a fully-equipped biology laboratory in a recent demonstration at the Chicago Undergraduate Division of the University of Illinois. Physics Professors Ora L. Railsback and Harold M. Skadeland presented the revolutionary design in school laboratories in the form of a full-scale, working model at Navy Pier. The key to the quick change is a built-in, automatically rotated turntable at each student station which delivers one set of lab equipment "on stage" while a previous set disappears into the wall. All units can be rotated at once or each one singly from a centrally operated electronic panel.

The new design thus allows a single laboratory to serve a variety of study courses—physics, biology, geology and others. This is a welcome economy for schools and colleges facing inflated building costs, Railsback and Skadeland believe.

Its most obvious advantage is that

while one section is in use in the laboratory, the other sections can be loaded with equipment from a behind-the-scenes storage room. This contrasts with conventional school laboratories that often are taken out of use for a full day each week to be re-equipped.

The professors presented a small scale model for the first time last June to the building committee of the American Physics Teachers' Association. Committee members asked tough questions about the new design, but were satisfied with the answers. The potentials for saving time, space and money were obvious.

Professors Railsback and Skadeland then went ahead with the full-size, working model. Built by Hamilton Manufacturing Company of Two Rivers, Wisconsin, the new lab, described as "still experimental" by its designers, features two distinct types of student stations and turntables, each with its particular set of advantages.

One grouping consists of a single, long laboratory bench with the series of turntables built into the wall above it. This permits a massive loading and unloading of units behind the wall.

In the other grouping the units are set up individually at right angles to the wall. The turntables are loaded from within the classroom itself, not from a hidden storage area. The time factor in loading was not seen as critical in the use of these units where the labs may be vacant for longer periods. They are particularly adaptable to research work of a continuing nature.

The relative merits of both types of units are yet to be determined through further study, according to Dr. Railsback.

With either type unit, equipment used in experiments of a continuing nature does not have to be dismantled at the close of each laboratory period and reassembled at the start of the next. Instead, the equipment simply disappears into the turntable between sessions.

It is conceivable that three continuing experiments could be carried on at each student station by three different student classes.

The new design also remedies the cluttered, disorganized appearance, usually found in advanced and graduate class labs. And, of course, the speed with which the lab can be converted provides students and teachers alike with more total time for experimentation.

Each station is equipped with water faucet and drain and electrical outlets with variable voltage outputs. The elaborate electrical circuits feed into a large, futuristic "switchboard."

"Rising student enrollments are going to tax the ingenuity of every scholastic institution to make the maximum use of available space," Dr. Railsback declared. "We think our new laboratory design is a positive step in that direction."

New TV Lens.—A new television lens—technically known as a Studio Varotal Zoom Lens—has been developed in Britain as the result of close collaboration between the BBC and Taylor, Taylor and Hobson (a division of Rank Precision Industries Ltd.), pioneers in this field.

It enables cameramen to make gradual changes between panoramic views and magnified close-ups without moving the camera and without losing any quality of definition.

Designed specifically to cater to the peculiarities of the television camera, and said to be a great technical advance, the lens was first used to televise Queen Elizabeth's Christmas Day address.

The full value of zoom lenses can only be obtained if they provide as

V.2
195

good quality definition as normal lenses which they replace.

This requirement presents severe optical and mechanical difficulties. Taylor Hobson overcame these difficulties for outside television broadcasting some years ago. They produced a zoom lens—the Outside Broadcast Varotal model—that in the past six years has become internationally accepted.

When similar results are required in the restricted space of an indoor television studio, the problems increase greatly. An Outside Varotal is not generally suitable for these conditions. The new Studio Varotal was designed to meet the worldwide demand for a zoom lens for studio use.

This is suitable for use with both image orthicon and vidicon camera tubes, interchangeable rear units being provided to suit the two formats. The focal length range of the Studio Varotal is 2¼ in. to 8 in. when fitted on image orthicon cameras and 2.25 cms. to 8 cms. on vidicon cameras.

The lens will focus down to 5 ft., which is unusually close for a zoom lens. These features have been provided while maintaining adequate reltive aperture and high standard of definition.

The optical design of the Studio Varotal has been specially developed to yield the type of performance demanded by television transimssion channels. The correction of all lens aberrations matches the spectral sensitivity of the television camera tube, and aberrational compensation has been provided for errors introduced by the face of the tube.

From the mechanical point of view, the lens has been designed to fit existing camera turrets with a minimum of adaptation. The three controls—focus, zoom and iris—take the form of gear rings mounted towards the rear of the lens, facilitating the fitting of either manual or servo drives.

Camera controls for the lens used during the Queen's broadcast were specially developed by the Engineering Division of the BBC. The lens is operated by a capstan on the right-hand side of the camera. This rotates for focusing and slides backwards or forwards for zooming, enabling the cameraman to perform the whole operation with one hand.

Oscar Fisher Company Unveil New Automatic X-Ray Processor.—The Oscar Fisher Company, of Newburgh, N. Y., have developed a new automatic processor, the Fisher FaX-Ray Processor.

The new unit, entirely automatic in operation, develops, fixes, washes and dries X-ray film of all sizes, up to and including 14 in. by 17 in. One of the unique features of this new apparatus is that the film transport is accomplished without making use of cumbersome, old-fashioned hangers.

Present methods of processing X-ray film require a minimum of one hour. The Fisher FaX-Ray Processor will make available to doctors completely dry X-rays in a matter of only 7 minutes. In critical surgical operations and emergency treatments in the nation's hospitals, the increased rate of processing, due to the use of a FaX-Ray Processor, will undoubtedly help the pathologist to save lives and relieve pain and suffering.

The FaX-Ray Processor also reduces the dosage required for X-ray diagnosis, allowing doctors ample time to examine films at leisure rather than subjecting patients to continuous X-ray or fluorography.

The FaX-Ray Processor is fabricated entirely of type 316L stainless steel. This is the only one of 42 differ-

ent types that satisfactorily resists the corrosive attacks of photographic chemicals. All seams are Heliarc welded and surfaces passivated.

X-ray films are developed in the FaX-Ray Processor by the Fisher method of agitation-immersion. Washing, too, is speeded up by a spray-thru-air system, after which X-ray films are dried by turbulent, filtered air and delivered automatically in only 7 minutes.

The Fisher FaX-Ray Processor can be operated by anybody and does not require photographic or technical training of any kind. Because the unit is entirely automatic, the operator after ten minutes of instruction, has only to check the proper temperatures of the solutions before setting the FaX-Ray Processor into operation. The 12-film automatic feed magazine is loaded in a darkroom with exposed film, from where it is transported automatically through a pass-thru chute to the FaX-Ray Processor in an adjacent room. Placing the FaX-Ray unit outside the darkroom permits the operator to work at peak efficiency and accuracy under daylight conditions.

Approximate dimensions of the Fisher FaX-Ray Processor are: length, 6 ft.; height, 7ft.; width, 4 ft.; and weight about 500 lb. (dry).

V.2
195